UNIVERSITÀ DEGLI STUDI DI MILANO

Scuola di Dottorato in Scienze Biologiche e Molecolari

XXVI Ciclo

ACA12 is a deregulated isoform of plasma membrane Ca^{2+}-ATPase of *Arabidopsis thaliana*

Margherita Limonta

PhD Thesis

Scientific tutor: Professor M.I. De Michelis

Academic year: 2012-2013

SSD: BIO/04

Thesis performed at:

Department of Life Science, University of Milan

Contents

Contents

Part I

Contents

Part II

Limonta M, Romanowsky S, Olivari C, Bonza MC, Luoni L, Rosemberg A, Harper JF, De Michelis MI (2013) Plant Molecular Biology. Epub ahead of print.

ACA12 is a deregulated isoform of plasma membrane Ca^{2+}-ATPase of *Arabidopsis thaliana.*

Part I

Abstract

Several environmental and endogenous stimuli activate plant signal transduction pathways through transient increases in cytosolic free calcium concentrations ($[Ca^{2+}]_{cyt}$). Strong evidence indicates that plant response specificity is triggered by the amplitude, shape, frequency and localization of these stimulus-induced Ca^{2+} oscillations. Due to their role in Ca^{2+} efflux from the cytosol, plant auto-inhibited Ca^{2+}-ATPases (ACAs) are involved in restoring the cytosolic basal concentration of Ca^{2+} after its rise due to stimulus perception, therefore affecting the specificity of plant response to different stimuli. Ten ACA isoforms are present in *Arabidopsis thaliana*, which are divided into four clusters based on gene structure and sequence homology. Cluster I, II and IV ACAs share a common mechanism of regulation based on a N-terminal auto-inhibitory domain whose action is suppressed by the interaction with the Ca^{2+}-sensor protein calmodulin (CaM). Cluster III isoforms (ACA12 and ACA13) compared to the other ACAs, are almost unknown and show unique features at sequence and expression levels: in particular ACA12 and ACA13 show divergences in residues involved in CaM binding and regulation while the expression levels, normally very low, are increased upon exposure to pathogens or UV stresses.

By confocal microscopy, a GFP-tagged ACA12 (expressed in Arabidopsis plants) was localized at the plasma membrane (PM). ACA12 was then expressed in *Saccharomyces cerevisiae* strain K616, which lacks endogenous Ca^{2+} pumps. Our results reveal that ACA12 allows the grow of K616 in a Ca^{2+}-depleted medium, therefore indicating that it is a functional and deregulated Ca^{2+} transporter. Yeast-expressed ACA12 was then purified by CaM-affinity chromatography and its activity was tested *in vitro* in order to study its biochemical properties. Biochemical assays results show that ACA12 is a functional Ca^{2+}-ATPase. Moreover, as expected, its activity is not regulated by CaM. Finally, in order to try to explain ACA12 deregulated behaviour, single point mutants of ACA12 were generated and tested for K616 phenotype complementation.

Taken together our results show that ACA12 has unique biochemical features suggesting for it a distinctive physiological role within the ACA family. In particular ACA12 may be involved in Ca^{2+}-dependent signaling pathways in response to plant specific stresses such as pathogens and UV.

Introduction

Ca^{2+} homeostasis in plant cell

Calcium ion (Ca^{2+}) is an essential plant nutrient employed by the cell for a wide range of structural and enzymatic functions. In particular Ca^{2+} is required for maintaining cell wall integrity and membranes structure and permeability [Hirschi, 2004; Hepler, 2005]. Moreover, it is well known that Ca^{2+} ion is a second messenger in numerous plant signaling pathways, where Ca^{2+} messages take the form of transient increases in cytosolic free ion concentration ($[Ca^{2+}]_c$). Elevations in $[Ca^{2+}]_c$ occur indeed during the transduction of a wide variety of stimuli such as abscisic acid (ABA), gibberellins, nodulation factors (NodF), bacterial and fungal elicitors, red/blue and UVB light, salt, drought, oxidative stresses and temperature signals [Sanders et al., 1999; McAinsh and Pittman, 2009; De Falco et al., 2010].

Due to its ability to form different coordination bonds (commonly six to eight), Ca^{2+} can easily interact with proteins, lipids and organic acids becoming, at high concentration, a toxic compound. It is therefore able to trigger protein and nucleic acids aggregation and to affect cell phosphate-based metabolism forming insoluble precipitates with orthophosphate (P_i). For this reason plant cells have to maintain low free $[Ca^{2+}]_c$ (around 100-200 nM), against millimolar values of external calcium levels [Sanders et al., 1999; Bose et al., 2011; Spalding and Harper, 2011]. Since Ca^{2+} cannot be metabolized like other second messenger molecules, plant cells tightly regulate cytosolic Ca^{2+} levels through Ca^{2+}-binding proteins and transporters. Most of calcium ions which enter in the cytosol during Ca^{2+}-mediated signals are rapidly sequestered by several Ca^{2+} binding proteins which markedly reduce free $[Ca^{2+}]_c$ and decrease the ion effective diffusion coefficient in the cytosol [Sanders et al., 1999; Hirschi 2004].

Beyond the buffering system of Ca^{2+}-binding proteins, cellular Ca^{2+} homeostasis is covered by a complex net of passive and active transporters localized both in the plasma membrane (PM) or in endomembranes. It is indeed known that all the intracellular organelles act as Ca^{2+} storage compartments (**Fig.1**); in particular vacuoles, thanks to their size and storage capacity, represent the most prominent intracellular sink for Ca^{2+} in plants. However, since buffering system and intracellular sequestration have finite capacities, cytosolic Ca^{2+} homeostasis is largely achieved at the expense of PM Ca^{2+} efflux systems which catalyze calcium transport toward the apoplast [Sanders et al., 1999; Stael et al., 2012].

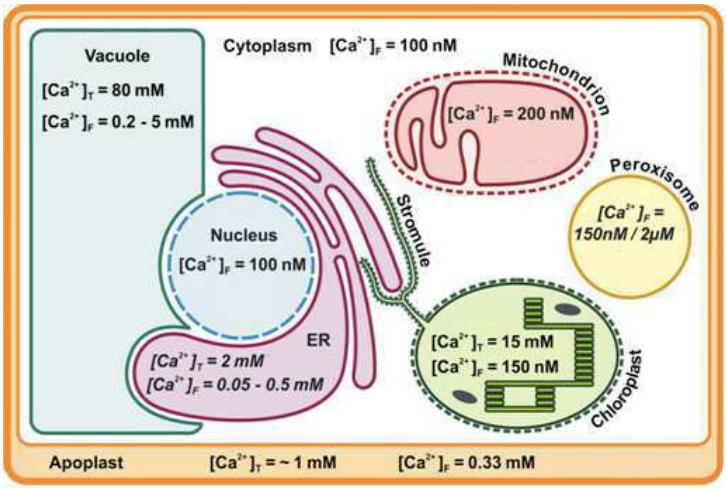

Fig.1 *Organellar Ca^{2+} concentrations in the plant cell.*
Values for reported total ($[Ca^{2+}]_T$) and free resting ($[Ca^{2+}]_F$) Ca^{2+} concentrations in the different organelles (apoplast, cytoplasm, vacuole, nucleus, ER, chloroplast, mitochondrion, and peroxisome).
From Stael et al., 2012

A negative cytosolic electrical potential (-150 mV) and a 10^4 difference in Ca^{2+} concentration (out/in) across the plasma membrane, result in an electrochemical potential difference for calcium ($\Delta\mu_{Ca}$) of -50 kJ mol^{-1}, meaning that Ca^{2+} may flow into the cytosol through passive transporters (such as ion channels) without energy costs. The same goes for Ca^{2+} ions stored in intracellular compartments, although the potential difference across the endomembranes is likely to be less negative than that across the PM. This highly negative $\Delta\mu_{Ca}$ enables the generation of quick 10-20 fold elevations in free $[Ca^{2+}]_c$ that function as an intracellular signal. By contrast, efflux of Ca^{2+} from the cytosol is mediated by active transporters, which restore Ca^{2+} resting conditions, powered either by ATP hydrolysis or by the counter transport of another cation [Sanders et al., 1999; Spalding and Harper, 2011].

As mentioned above, Ca^{2+} is involved in a multitude of plant physiological processes; the versatility of this intracellular second messenger encouraged investigations on how specificity is encoded in calcium-based signalling system. Several mechanisms have emerged that may contribute to specificity in Ca^{2+} signaling among which the availability of a specific set of Ca^{2+} sensors (and downstream target proteins) and the interplay with other intracellular messengers that can modulate the Ca^{2+} signaling. However, advances in Ca^{2+} dynamics monitoring techniques (during the last 30 years), unraveled that the

specificity of a Ca^{2+} signal is strongly correlated to spatio-temporal patterns of $[Ca^{2+}]_c$ elevation. In this way, the stimulus induced by specific signals is propagated into the cytosol as waves of Ca^{2+} that can differ for duration, frequency, amplitude and spatial localization. This spatial and temporal dynamic of $[Ca^{2+}]_c$ elevations is called "Ca^{2+} signature" and proceeds from the balance between ion influx and efflux, together with the buffer activity of Ca^{2+}-binding proteins. In the light of this mechanism, the expression, activity and regulation of the complex net of proteins that transport Ca^{2+} uphill and downhill across membranes, become crucial in finely modulating the Ca^{2+} signature, thus contributing to generate specificity in Ca^{2+}-mediated messages [Evans et al., 2001; Hetherington and Brownlee 2004; McAinsh and Pittman, 2009; Spalding and Harper, 2011].

Generation of Ca^{2+} signals: influx systems

The generation of stimulus-specific $[Ca^{2+}]_c$ elevations is associated in plants with the opening of Ca^{2+}-permeable cations channels, releasing calcium from both the apoplast and intracellular compartments. These channels can be classified as voltage-gated or ligand-gated based on their activation mechanism [Rudd and Franklin-Tong, 2001; Kudla et al., 2010].

Electrophysiological studies identified in the plasma membrane two type of voltage-gated channels: depolarization-activated Ca^{2+}-permeable channels (DACCs) and hyperpolarization-activated Ca^{2+}-permeable channels (HACCs). DACC channels are permeable to both monovalent and divalent cations and are presumably involved in transducing stress-related signals; in particular a specific role has been proposed in plant response to chilling and microbe interaction. Instead HACC channels, permeable to many divalent cations, are activated both by blue light and ABA and play a crucial role in stomatal regulation. Although the properties of DACCs and HACCs are well studied electrophysiologically, the molecular identity of these channels is still unknown [Sanders et al., 2002; White and Broadley, 2003; Kudla et al., 2010].

Two classes of non-selective ligand-gated channels are also present in the plasma membrane: cyclic nucleotide-gated channels (CNGCs) and glutamate receptor-like channels (GLRs). CNGC channels (20 isoforms in Arabidopsis) are activated by the binding of cAMP or cGMP to a CNB (cyclic nucleotide binding) domain, in the C-

terminal portion of the protein. Their activity is inhibited through a feedback mechanism based on the interaction between Ca^{2+} and the calcium-sensor protein calmodulin (CaM); the Ca^{2+}-CaM complex binds a CaM-binding site, which overlaps the CNB domain, reducing the affinity of the cyclic nucleotide for its site. GCNC channels have been shown to be involved in Ca^{2+}-mediated response to pathogens, ion homeostasis regulation during salt stress adaptation and tip growth of pollen tubes. Conversely, glutamate receptors-like channels (GLRs, 20 isoforms in Arabidopsis) are activated by several amino acids like Glu and Gly. It is assumed that GLRs are involved in plant Ca^{2+} nutrition and in mediating Ca^{2+}-response upon cold stress, but they are also implicated in the regulation of many different developmental aspect such as hypocotyl elongation, maintenance of cell division, and pollen tube growth and morphogenesis [Kudla et al., 2010; Spalding and Harper, 2011; Jammes et al., 2012].

There are evidences of ligand- or voltage-dependent Ca^{2+} release also in plant endomembranes. Several electrophysiological studies support the existence of ligand-gated channels at the tonoplast, suggesting for these channels an inositol 1,4,5-trisphosphate ($InsP_3$)- or a cyclic ADP-ribose (cADPR)-dependent activation. Both $InsP_3$ and cADPR have been shown to be implicated in multiple Ca^{2+}-mediated stress signaling pathways such as transduction of salt and hyperosmotic stress signals or activation of plant defence genes and ABA signal transduction. The only ligand-gated channel that appears to reside in the endoplasmic reticulum (ER) membrane is activated by NAADP (nicotinic acid adenine dinucleotide phosphate), however, also in this case, the molecular identity of the channel is still unknown. Another tonoplast-resident channel type is the slow vacuolar (SV) channel, recently associated to the protein TPC1 (two-pore channel 1) in Arabidopsis. SV channel is gated by membrane depolarization and seems to be regulated by Ca^{2+} in two opposite ways: it is indeed activated by increased $[Ca^{2+}]_c$, while an increase in the vacuolar Ca^{2+} concentration inactivates the channel. In Arabidopsis, TPC1 channel results involved in the pathogen-resistance signaling pathway [Sanders et al., 2002, White and Broadley, 2003; McAinsh and Pittman, 2009; Kudla et al., 2010; Spalding and Harper, 2011].

According to their activation and regulative properties these channels can modulate the Ca^{2+} signature affecting ion influx parameters.

Generation of Ca^{2+} signals: efflux systems

Efficient mechanisms of Ca^{2+} efflux, removing ion excess from the cytosol, are crucial in both keeping $[Ca^{2+}]_c$ at submicromolar level and in reloading Ca^{2+} stores after Ca^{2+} signaling is completed. However, in addition to their housekeeping functions, these efflux systems are also involved in modulating the dynamic of the calcium signature, therefore affecting the information encoded by the calcium signals [Sanders et al., 2002; Bose et al., 2011]. There are two groups of Ca^{2+} efflux system, Ca^{2+}-ATPases and Ca^{2+} antiporters, which provide active transport systems that move Ca^{2+} out of the cytosol using respectively the energy coming from the hydrolysis of ATP or the counter transport of another cation (usually H^+). While antiporters provide low-affinity (K_m= 10-15 μM) but high-capacity calcium transport, Ca^{2+}-ATPases are high-affinity (K_m=0,1-2 μM) but low capacity transporters, suggesting two different roles in restoring the basal $[Ca^{2+}]_c$. It is indeed assumed that antiporters reduce cytosolic Ca^{2+} levels back to few micromolar concentrations while pumps are important to achieve and finely tune the low resting concentration of Ca^{2+} in the cytosol [Bose et al., 2011; Kudla et al., 2010; Spalding and Harper, 2011].

In Arabidopsis genome, six genes encode for putative H^+/Ca^{2+} antiporters, also named cation exchangers (CAX), while five more genes, called cation/Ca^{2+} exchangers (CCX), resemble an animal Na^+/Ca^{2+} exchanger isoform. CAX isoforms reside on the tonoplast and show different ion specificity (beside Ca^{2+}, some isoforms appear to transport also Cd^{2+} and Mn^{2+}). They harbor an N-terminal regulatory/autoinhibitory domain, able to bind an adjacent region within the N-terminus. Other forms of regulation have been reported such as formation of heteromers, phosphorylation, pH and interaction with regulative proteins (such as the kinase SOS2). Recent analysis of Arabidopsis CAX knock-out mutants show increased sensitivities to abiotic stresses among which toxic metals, cold and salt stresses [Sanders et al., 2002; McAinsh and Pittman, 2009; Kudla et al., 2010; Manohar et al., 2011]. A H^+/Ca^+ antiport activity was also reported to reside at the plasma membrane and in the chloroplast thylakoid membrane, however it is possible that this activity is conferred by cation antiporters that are distinct from CAXs [Shigaki and Hirshi, 2006; Kudla et al., 2010].

On the other hand, plant Ca^{2+}-ATPases belong to the P-type ATPase superfamily, which directly use ATP to drive ion and lipid translocation across cellular membranes.

P-type ATPases

P-type ATPases are a large family of active transporters essential for almost all life forms. Indeed, members of this family generate and maintain crucial electro-chemical gradients across cellular membranes, translocating cations, heavy metals and lipids at the expense of ATP hydrolysis energy. Common biochemical characteristic of these pumps is the formation of a phosphorylated intermediate during the catalytic cycle which involves an Asp residue localized in the conserved consensus sequence DKTG [Palmgren and Axelsen, 1998; Axelsen and Palmgren, 2001].

Based on their phylogenetic analysis, the P-type ATPases can be divided into five groups (I-V) that differ in structural characteristics, transported substrate and organisms in which they are present. Each group can be further split into two or more sub-groups (A, B, C…). [Axelsen and Palmgren, 1998; Palmgren and Nissen, 2011; Pedersen et al., 2012].

Despite the low degree of sequence conservation, P-type ATPases (above all members of groups II and III) share a similar membrane topology characterized by the presence of 6-12 hydrophobic transmembrane helices (TM) and cytosolic N- and C-termini; they also exhibit two cytosolic-faced loops: a small loop (between TM2 and TM3) and a large central loop (between TM4 and TM5) [Axelsen and Palmgren, 2001; Kühlbrandt, 2004].

All we know about the 3D structure of P-type ATPases comes from the resolution of the crystal structure of group II and III pumps (the IIA Ca^{2+}-ATPase of rabbit muscle SERCA1a, the IIC Na^{+}-K^{+}-ATPase and the IIIA H^{+}-ATPase) which exhibit 10 TM. The general 3D structure is characterized by four functionally and structurally distinct domains (**Fig.2**). The cytosolic head of the enzyme is composed by the P-, the N- and the A-domains. The P-domain (Phosphorylation), localized in the large cytosolic loop, contains the Asp residue that is phosphorylated during the catalytic cycle by the N-domain (Nucleotide binding), which is a modular insertion into the P-domain that includes a conserved sequence motif identified as the nucleotide-binding site. Instead the A-domain (Actuator) is formed by the small cytosolic loop together with a portion of the N-terminus and plays a crucial role both in enzyme dephosphorylation and in regulating the mechanism of ion binding and release. Finally transmembrane α-elices form the M-domain (Membrane) which harbors the ion-binding site(s) embedded in the membrane [Kühlbrandt, 2004; Palmgren and Nissen 2011].

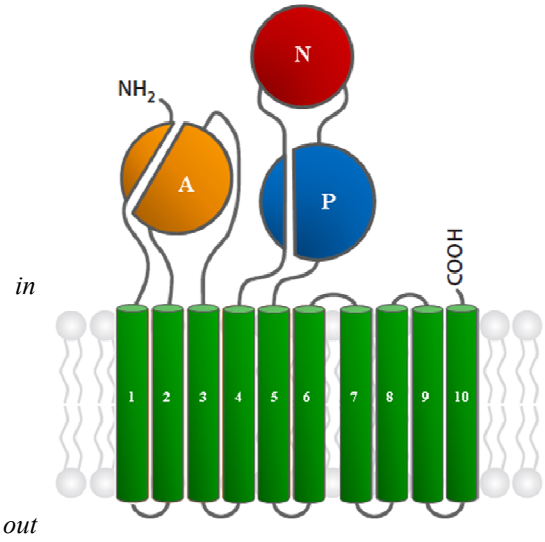

Fig.2 *Schematic diagram of the structural organization of a P-type ATPase (modeled on the crystal structure of the sarco-endoplasmic reticulum Ca^{2+} ATPase, SERCA1a).*
The pump is organized into three cytoplasmic domains (A, P, and N) and one membrane-embedded domain (M). The A-domain is formed by the small cytoplasmic loop together with a portion of the N-terminal region. The N-domain is an insertion into the P-domain, both of which are formed by the large cytoplasmic loop. The membrane-embedded region consists of 10 transmembrane-spanning segments.
From Palmgren and Nissen, 2011

ATP hydrolysis supplies the driving force for the ion transport across the membrane, causing large conformational changes of the enzyme structure. In particular, P-type ATPases switch between two main conformational states (E1 and E2) and two intermediate phosphorylated states (E1P and E2P) with different affinity for the transported ion. The resolution of SERCA1a crystal structure in different conformational states, validates the E1-E2 model of the P-type ATPases catalytic mechanism (**Fig. 3**), previously proposed based on detailed functional and biochemical studies [Toyoshima and Inesi, 2004; Kühlbrandt, 2004; Møller et al., 2005]. In the E1 state, the transmembrane ion-binding site, which faces the cytoplasm, has a high affinity for the transported ion. Ion-binding allows the interaction of ATP with its site in the N-domain and the subsequent phosphorylation of the Asp residue in the P-domain. This drives the enzyme in the phosphorylated intermediate E1P-ADP state during which the ion is occluded in the M-domain. Ion transfer toward the extracellular space occurs only after the transition to E2P state triggered by ADP release. As the ion is released into the extracellular space, in case of an antiporter activity of the pump, a counter-ion can enter the ion-binding site and the Asp residue undergoes dephosphorylation (E2 state). Finally,

the P_i is dissociated and the enzyme can revert to the E1 state in which the counter-ion is released into the cytoplasm and another cycle begins [Toyoshima et al., 2003; Toyoshima and Inesi, 2004; Møller et al, 2005; Niggli and Sigel, 2008; Bublitz et al., 2011; Bublitz et al., 2010; Chourasia and Sastry, 2012].

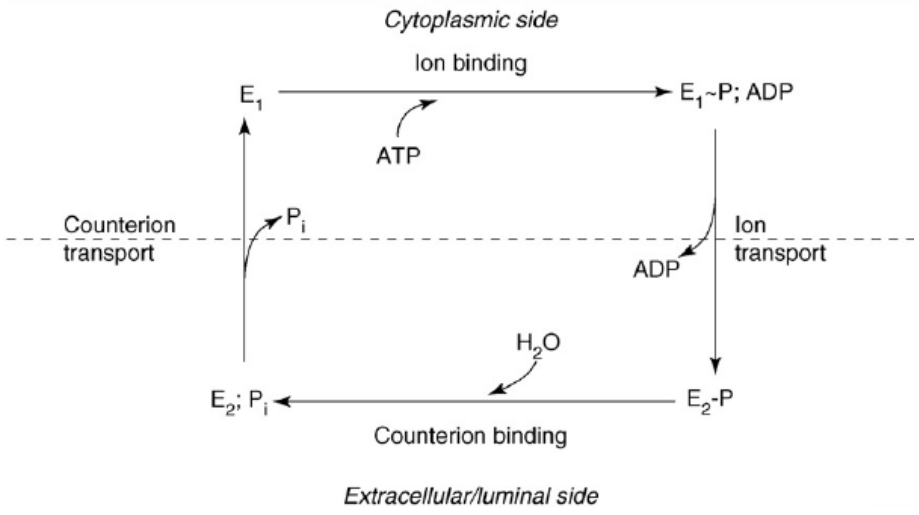

Fig.3 *A simplified scheme illustrating the E1–E2 model of P-type ATPases.*
P-type ATPases undergo large conformational changes during ion translocation. E1 and E2 correspond to two distinct major conformations which display different affinities for the transported ions. The pumping cycle involves several further intermediate states. Transport of the primary ion is associated with phosphorylation of the pump by ATP. Transport of the counter ion is associated with dephosphorylation of the pump.
From Niggli and Sigel, 2008

Plant Ca^{2+}-ATPases

Ca^{2+} pumps belong to sub-groups IIA and IIB of the P-type ATPases [Baxter et al., 2003]. IIA and IIB Ca^{2+}-ATPases (present in both animals and plants) share the essential P-type properties, among which membrane topology and reaction mechanism. However, these pumps also display significant differences, particularly related to transport stoichiometry, activity regulation and sensitivity to inhibitors [Sze et al., 2000; Brini and Carafoli, 2009; Bonza and De Michelis, 2011].

It is known that the number of Ca^{2+} binding sites varies among IIA and IIB pumps. Type IIA Ca^{2+}-ATPases indeed have two Ca^{2+} binding site in the M domain, only one of which is retained by IIB pumps. As a consequence, the first show a stoichiometry of two transported Ca^{2+} ions for each hydrolyzed ATP, whereas the second show a $1Ca^{2+}$/ATP

transport stoichiometry [Brini and Carafoli 2009; Bonza and De Michelis, 2011]. These pumps also have different specificities for the transported divalent cations: IIA pumps are able to transport Mn^{2+} and Zn^{2+}, beside Ca^{2+}, whereas IIB pumps are highly specific for Ca^{2+} [Sze et al., 2000; Baxter et al., 2003; Kabala and Klobus, 2005; Bonza and De Michelis, 2011]. Both IIA and IIB act as Ca^{2+}/H^{+} exchangers. Models based on the structures of the crystallized pumps suggest that the counter-transport may be a built-in characteristic of P-type ATPases. Effectively in case of Ca^{2+}-ATPases, it has been suggested that protons can compensate for the severe charge imbalance created in the Ca^{2+}-binding sites after Ca^{2+} release [Niggli and Sigel., 2008].

Both IIA and IIB pumps are sensitive to P-type ATPase common inhibitors like ortho-vanadate (a transition state analogue of inorganic phosphate) and lanthanum. However this latter inhibitor increases the steady state level of phosphorylated intermediate in IIB pumps, while decreases it in the other P-type including IIA pumps suggesting a different inhibitory mechanism [Brini and Carafoli, 2009; Palmgren and Nissen, 2011]. Moreover, IIA Ca^{2+}ATPases differ for their sensitivity to thapsigargin and cyclopiazonic acid (CPA), whereas IIB pumps are characterized by a high sensitivity to fluorescein derivatives (such as erythrosine B, and eosin Y) [Brini and Carafoli, 2009; Bonza and De Michelis, 2011].

In plant cells IIA and IIB Ca^{2+} pumps have been respectively called ECA (for ER-type Ca^{2+}-ATPase) and ACA (for auto-inhibited Ca^{2+}-ATPase) and have been localized both at the PM and at the endomembranes [Geisler et al., 2000a; Sze et al., 2000].

Common biochemical features of ECA pumps are a strong preference for ATP as nucleotide triphosphate substrate and high affinity for Ca^{2+} ($K_{0,5}$ in the submicromolar range). ECAs differ from their animal orthologue SERCA in being insensitive to thapsigargin, a plant derived compound which inhibits SERCA at sub-nanomolar concentrations. Little is known on ECAs regulation: the activity of SERCA is inhibited by the interaction with phospholamban, but neither phospholamban nor other proteins have been identified so far in plants as ECA regulators. [Brini and Carafoli, 2009; Pittman et al., 2010; Bonza and De Michelis, 2011].

In contrast to ECAs, activity regulation of ACA pumps have been widely studied (see below): ACAs differ from their animal orthologue PMCA by having the regulative domain localized at the N-terminal end of the protein rather than at the C-terminus. ACA isoforms characterized so far are unique among P-type ATPases for being able to use ITP and GTP as alternative substrate to ATP. Moreover, ACAs are also particularly sensitive

to inhibition by fluorescein derivatives which are known to bind the nucleotide binding site. Both low specificity for the nucleotide triphosphate and high sensitivity to fluorescein derivatives may correlate with a different conformation of the nucleotide binding site of ACA isoforms with respect to the other P-type ATPases [De Michelis et al., 1993; Bonza et al., 2004; Kabala and Klobus, 2005; Bonza and De Michelis, 2011].

Four ECA and ten ACA genes have been identified in *Arabidopsis thaliana* genome. Both ECA and ACA isoforms are divided into clusters based on sequence alignment and intron number and position, however several evidences indicate a correlation between clusters and intracellular localization [Baxter et al., 2003].

ECA isoforms can be divided in two clusters; cluster I groups ECA1, ECA2 and ECA4, whereas cluster II contains ECA3. Only isoforms 1 and 3 have been characterized in any detail. ECA1 was found localized at the ER while ECA3 has been associated with Golgi and post-Golgi vesicles membranes. Studies on Arabidopsis knock-out mutants for ECA1 and ECA3 genes suggest an involvement in Mn^{2+} stress tolerance and in Ca^{2+}/Mn^{2+} nutrition; eca3-/- knock-out mutant also show an altered protein secretion [Wu et al., 2002; Li et al., 2008; Pittman et al., 2010; Bonza and De Michelis, 2011].

Arabidopsis ACA isoforms are divided into four clusters. Cluster I comprehends ACA1, ACA2 and ACA7: while isoform 1 and 2 have been localized at the ER, the localization of ACA7 remains unknown. ACA4 and ACA11 belong to cluster II and are both localized in the tonoplast. Cluster IV groups isoforms ACA8, ACA9 and ACA10 which have been localized at the PM. Both cluster I and II isoforms are encoded by genes harboring 6 introns and cluster IV ACA isoforms share a complex gene structure characterized by more than 30 introns. Little is known so far about cluster III isoforms, ACA12 and ACA13, which are unique in being encoded by intron-less genes [Baxter et al., 2003; Pittman et al., 2010; Bonza and De Michelis, 2011; Kamrul Huda et al., 2013].

ACA pumps are deeply implicated in plant development. An evident knock-out phenotype has been identified in Arabidopsis for ACA9 and ACA7, which are primarily expressed in pollen. The knock-out mutant aca9-/- shows reduced pollen tubes growth which results in an high frequency of aborted fertilization and reduced seed set; conversely aca7-/- knock-out causes defect in pollen grain development resulting in a higher amount of dead pollen grains with respect to WT Arabidopsis plants [Schiøtt et al., 2004; Lucca and León, 2012].

Single aca8-/- Arabidopsis mutant displays no evident developmental phenotype under controlled conditions, by contrast aca10-/- mutant exhibits reduced inflorescence height and increased axillary stem formation: this phenotype is enhanced in aca8-/- aca10-/- double mutant plants which also display a reduced root growth when cultivated *in vitro* [Frei dit Frey et al., 2012]. Moreover, in the presence of a naturally occurring dominant allele of the CIF2 unlinked gene, aca10 -/- knock-out line displays altered adult vegetative growth and inflorescence elongation [George et al., 2008]. Both these phenotypes are complemented by the overexpression of the ACA8 isoform in the knock-out plants suggesting a partially functional redundancy between isoform 8 and 10.

ACA isoforms are also involved in ABA response. In *Egeria densa* leaves, ABA rapidly induces an increase in the activity of a PM localized ACA; moreover in *Arabidopsis thaliana* seedlings, ABA treatment increases the transcription of ACA8 and ACA9 (which correlates with an increased ACA8 protein amount) [Beffagna et al., 2000; Cerana et al., 2006].

Several evidences also suggest an involvement of ACAs in response to specific stresses: the expression of ACA8 in Arabidopsis guard cells is upregulated upon cold treatment, whereas the over-expression of ACA2 and ACA4 improves salt tolerance in yeast suggesting a role also in plant response to salt stress [Schiøtt and Palmgren, 2005; Geisler et al., 2000b; Anil et al., 2008].

Finally ACA pumps are also involved in pathogen response. It is known that, in Arabidopsis cultured cells, PM-localized Ca^{2+}-ATPases activity is stimulated upon exposure to the fungal elicitors oligogalacturonides (OG) [Romani et al., 2004]. In Arabidopsis, a double knock-out mutation of the vacuolar Ca^{2+} pumps ACA4 and ACA11 leads to a high frequency of apoptosis-like lesions resulting from the activation of the salicylic acid-dependent programmed cell death pathway [Boursiac et al., 2010]. Moreover it has been recently shown that ACA8, transiently expressed in *Nicotiana bentamiana* leaves, specifically interacts with FLS2, the receptor for the bacterial elicitor flagellin (flg22). In addition both aca8-/- and aca10-/- knock-out Arabidopsis lines and the aca8-/- aca10-/- double knock-out mutant are more susceptible to bacterial infections [Frei dit Frey et al., 2012].

Regulation of ACA

Whereas ECAs seem to be involved principally in delivery of cations to intracellular compartments (where there is a requirement for secretion or as a cofactor for enzymatic activity), ACA pumps, due to their distinctive features, are emerging as potential key players in plant Ca^{2+} signaling. Therefore the biochemical characterization of the activity and regulation of different isoforms is crucial in dissecting the molecular basis of Ca^{2+}-mediated signaling pathways [Dodd et al., 2010].

The activity of ACA pumps is modulated by an N-terminal localized autoinhibitory domain (**Fig. 4**) which keeps the pump in a low activation state interacting with its catalytic head. Regulatory properties of ACA isoforms have been widely studied exploiting ACA8 isoform, the best characterized PM-localized ACA [Bonza et al., 2000].

The removal of the N-terminal region of ACA8 (through controlled proteolysis or genetic deletion) generates a deregulated (constitutively active) protein. Alanine scanning of the Arg^{43}-Lys^{68} sequence of ACA8 allowed the identification of six amino acids (Trp^{47}, Arg^{48}, Leu^{52}, Asn^{55}, Arg^{58} and Phe^{60}) important for pump autoinhibition (**Fig. 5**), with mutation of any of these residues resulting in a partially deregulated enzyme. However, it has been demonstrated that the autoinhibitory domain extends beyond this region: in fact the deletion of the first 100 or more N-terminal amino acids of ACA8 leads to an higher enzyme activity compared to the deletion of the first 74 amino acids [Luoni et al., 2004; Bækgaard et al., 2006].

A region in the small cytoplasmic loop of ACA8, between Glu^{268} and Trp^{348}, has been identified as one of the potential intramolecular partners of the autoinhibitory domain (**Fig. 4**): a peptide reproducing this sequence is indeed able to bind ACA8 N-terminus in pull-down experiments. Six acidic residues were identified in this region as important for the autoinhibitory mechanism, indeed mutation of each of them leads to a partially deregulated enzyme. These results suggest that the interaction of the N-terminal region with this portion of the small cytoplasmic loop is, at least partially, responsible for pump autoinhibition. Moreover it has been proposed that the presence of acidic negative-charged residues in the small cytoplasmic loop could be relevant in stabilizing the interaction with the autoinhibitory N-terminal domain, that is, instead, rich in basic residues [Luoni et al., 2004; Bækgaard et al., 2006; Fusca et al., 2009].

Three other acidic residues, localized at the cytosolic edge of TM1, TM2 and TM3 (stalk domain), were found to be crucial for enzyme autoinhibition. These residues were

originally identified in the ER-localized ACA2 isoform as Glu^{167}, Asp^{219} and Glu^{341}; mutation of each of them results in a fully deregulated pump. A highly conservative substitution at Asp^{219} ($D^{219}E$) still produces a deregulated enzyme suggesting for this amino acidic position a high sensitivity to perturbation [Curran et al., 2000]. Indeed, of the three amino acids, the Asp^{219} appears to be the most highly conserved among IIA and IIB pumps. Indeed the relevance of this Asp residue was confirmed also in other pumps: mutations of Asp^{170} in PMCA and Asp^{239} in ACA8 also determines a loss in pump autoinhibition [Bredeston and Adamo, 2004; Fusca et al., 2009]. A careful characterization of the $D^{170}N$ mutant PMCA suggested that the autoinhibitory domain was not displaced by the mutation, but rather that the increased pump activity may arise from directly changing the accessibility of the Ca^{2+}-binding site [Bredeston and Adamo, 2004; Corradi and Adamo, 2007].

The autoinhibitory action can be suppressed by several mechanisms, among which the interaction with the activator protein calmodulin (CaM) is the most widely studied [Sze et al., 2000; Bonza et al., 2013].

CaMs are acidic proteins of ~17 kDa with a Ca^{2+}-sensor function. Their structure is characterized by two globular domains connected together by an highly mobile extended α-helix; the globular domains consist of two EF-hands motifs each of which binds a Ca^{2+} ion. Ca^{2+}-binding to CaM, occurring with positive co-operativity, induces large conformational changes which result in the exposure of hydrophobic regions, available for downstream target interaction. Although there does not exist a real consensus sequence for the CaM-binding domain (CaM-BD), it usually consists of 15–30 basic amino acids sequence and has a tendency to form an anphypatic α-helix structure [James et al., 1995; De Falco et al., 2010; Zielinski et al., 1998].

Two N-terminal localized CaM-BD sites were identified in ACA8 (**Fig. 4**) partially overlapped to the autoinhibitory region. The first CaM-BD, with high affinity for CaM (Kd~13-26 nM), is localized in the region from Arg^{43} to Lys^{68} and is defined by the two CaM anchor residues Trp^{47} and Phe^{60}. Besides these two anchor residues, 11 other hydrophobic or basic residues (Arg^{48}, Ala^{51}, Val^{53}, Leu^{54}, Ala^{56}, Arg^{58}, Arg^{61}, Leu^{64}, Lys^{67} and Lys^{68}) were found to be important for the stability of the complex between CaM and the CaM-BD (**Fig. 5**) [Bækgaard et al., 2006].

The second CaM-BD of ACA8 has low affinity for CaM (Kd 500 nM) and is defined by the two hydrophobic residues Ile^{79} and Phe^{92} [Tidow et al., 2012].

The regulative model proposed suggests that at basal $[Ca^{2+}]_c$, the autoinhibitory domain interacts with its intramolecular target keeping the pump in a low activation state by blocking the substrate binding site or by preventing the conformational rearrangements required for the catalytic cycle. Once $[Ca^{2+}]_c$ arises CaM binds Ca^{2+} and undergoes conformational changes which make it able to interact with its CaM-BDs. CaM binding discards the interaction of the autoinhibitory domain with the catalytic head of the enzyme: this leads to pump activation both increasing V_{max} and decreasing the its $K_{0,5}$ for free Ca^{2+} [Rasi-Caldogno et al., 1993; Bækgaard et al., 2006]. The presence of two CaM-BDs with different affinity for the Ca^{2+}-CaM complex suggests that the CaM-dependent activation of the pump has a biphasic mechanism which would allow the modulation of the pump activity over a broad range of $[Ca^{2+}]_c$ [Tidow et al., 2012].

ACA8 is also activated by acidic phospholipids by two distinct mechanisms, involving their binding to two different sites. APL binding to a site overlapping the first CaM-BD, stimulates ACA8 activity similar to CaM, while binding to a second site (yet unidentified) provides a further stimulation of ACA8 activity by lowering its $K_{0.5}$ for free Ca^{2+} [Bonza *et al.*, 2001; Meneghelli et al., 2008].

Finally ACA8 activity is also regulated by phosphorylation: six Ser residue localized in the N-terminal region were found phosphorylated in large-scale phospho-proteomic studies. It has been shown that mimicking phosphorylation on these six Ser residue (through an S to D mutation) affects enzyme activity both by hampering the autoinhibitory function and changing the affinity for CaM. It is also shown that the ACA8 N-terminus is phosphorylated *in vitro* by two isoforms of *A. thaliana* CDPK, CPK1 and CPK16: in particular CPK16, the more efficient of the two isoforms tested, phosphorylates the ACA8 N-terminus at two different serine residues (Ser^{19} and Ser^{22}) [Giacometti et al., 2012]. Phospho-regulation has been studied also on other ACA isoforms. Two Ser residues in the N-terminus of the *Brassica oleracea* tonoplast isoform BCA1, one of which within the CaM-BD, can be phosphorylated *in vitro* by the protein kinase C (PKC) [Malmström et al., 2000]. Also the ER isoform ACA2 is target of *in vitro* phosphorylation: a calcium-dependent protein kinase (CDPK, isoform CPK1) can inhibit the basal and calmodulin-stimulated activities of the Ca^{2+} pump through phosphorylation on a serine residue just downstream the CaM-binding site [Hwang et al., 2000].

It is therefore possible that various ACAs are differently regulated by phosphorylation of N-terminal residues. Indeed the amino acidic sequence of the N-terminal regulative region, is the most variant within the ACAs and the serine residues found phosphorylated in ACA2 and ACA8 are not generally conserved among the ACA isoforms.

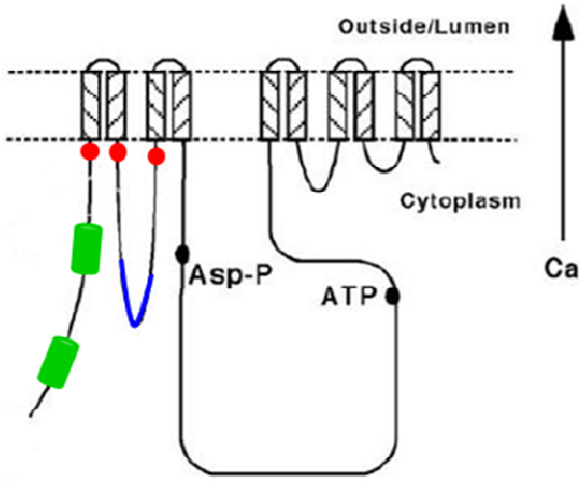

Fig.4 *Topology model for a typical plant ACA.*
The CaM-regulated autoinhibitor domain is located at the N-terminal end partially overlapped with two CaM-BDs (green barrels).The intramolecular site for the N-terminal autoinhibitory domain is marked in blue in the small cytoplasmic loop. Three residues (red dots) are localized at the cytosolic edge of TM1, TM2 and TM3 (Glu^{167}, Asp^{219} and E^{341} in ACA2): mutation of these residues results in a fully deregulated pump. The sites of the phospho-Asp and ATP binding are marked in the large cytoplasmic loop.
From Boursiac and Harper, 2007; modified

Aim of the work

Unlike the other ACAs, cluster III isoforms (ACA12 and ACA13) show distinctive features suggesting for these pumps highly different regulatory properties. Indeed the sequence of their N-terminal region is highly divergent compared to those of other ACAs (**Fig. 5**). In particular, the CaM-BD lacks several residues found to be important for CaM binding and stabilization, among which also one of the two CaM anchor-residues suggesting lower or no affinity for the activator protein CaM. Moreover, in the small cytoplasmic loop (at the cytosolic edge of TM2 and TM3), two of the three acidic residue known to be crucial for pump autoinhibition (identified as Asp^{219} and Glu^{341} in ACA2), which are strictly conserved among IIB Ca^{2+} pumps, are naturally variant in cluster III isoforms (Asn^{211} and Arg^{334} in ACA12, **Fig. 5**). These features suggest that ACA12 and

ACA13 may have lost the regulatory mechanism based on pump autoinhibition [Boursiac and Harper, 2007].

(A)

```
ACA1        11 DVKPKNSSDEALQRWRKLCWIVKNPKRRFRFTANLSKRSEAEAIRRSNQEKFRVAVLVSQ  70
ACA2        10 DVKAKHSSEEVLEKWRNLCGVVKNPKRRFRFTANLSKRYEAAAMRRTNQEKLRIAVLVSK  69
ACA7        10 DVKAKHSSEEVLEKWRNLCSVVKNPKRRFRFTANLSKRYEAAAMRRTNQEKLRIAVLVSK  69
ACA4         9 EVEAKNPSLEARQRWRSSVSIVKNRTRRFRNIRDLDKLADYENKKHQIQEKIRVAFFVQK  68
ACA11        9 EVASKNPSLEARQRWRSSVGLVKNRARRFRMISNLDKLAENEKKRCQIQEKIRVVFYVQK  68
ACA8        34 IPS-KNASIERLQQWR-KAALVLNASRRFRYTLDLKK----EQETREMRQKIRSHAHALL  87
ACA9        47 IDNTKNASVESLRRWR-QAALVLNASRRFRYTLDLNK----EEHYDNRRRMIRAHAQVIR 101
ACA10       33 IASTKNAPVERLRRWR-QAALVLNASRRFRYTLDLKR----EEDKKQMLRKMRAHAQAIR  87
ACA12       14 LNLTTSSLNKAQRRWR-FAYAAIYSMR---AMLSLVK----EIVPARIDPKTSDASLSLS  65
ACA13       20 LLELPKTLSKSNKKWQ-LALIKLYCSR---TLLNCAK----HAIRK---PGLFPRSLSYT  68
```

(B)

```
ACA1       203 GLGIVASILLVVFVTATSDYRQSLQFKDLDAEKKKIVVQVTRDKLRQKISIYDLLPGDVV 262
ACA2       201 GLGIAASILLVVFVTATSDYRQSLQFRDLDKEKKKITVQVTRNGFRQKLSIYDLLPGDIV 260
ACA7       202 GLGIVASILLVVFVTATSDYRQSLQFRDLDKEKKKITVQVTRNGFRQKMSIYDLLPGDVV 261
ACA4       198 GTGILLSILLVVMVTAISDYKQSLQFRDLDREKKKIIVQVTRDGSRQEISIHDLVVGDVV 257
ACA11      198 GTGILLSIILVVMVTAISDYKQSLQFRDLDREKKKIIIQVTRDGSRQEVSIHDLVVGDVV 257
ACA8       221 GGSIAFAVILVIVVTAVSDYKQSLQFQNLNDEKRNIHLEVLRGGRRVEISIYDIVVGDVI 280
ACA9       235 GGSIAFAVLLVIVVTAVSDYRQSLQFQNLNDEKRNIQLEVMRGGRTVKISIYDVVVGDVI 294
ACA10      221 GISIAFAVLLVIVVTATSDYRQSLQFQNLNEEKRNIRLEVTRDGRRVEISIYDIVVGDVI 280
ACA12      193 GGSIFVAVFLVIVVSALSNFRQERQFDKLSKISNNIKVEVLRDSRRQHISIFDVVVGDVV 252
ACA13      188 GGSIFVAVFLVVAVSAVSNFRQNRQFDKLSKVSSNIKIDVVRNGRRQEISIFDIVVGDIV 247


ACA1       322 TVGMRTQWGKLMATLSEGGDDETPLQVKLNGVATIIGKIGLFFAVITFAVLVQGLAN--- 378
ACA2       320 TVGMRTQWGKLMATLTEGGDDETPLQVKLNGVATIIGKIGLFFAVVTFAVLVQGMFM--- 376
ACA7       321 TVGMRTQWGKLMATLSEGGDDETPLQVKLNGVATIIGKIGLSFAIVTFAVLVQGMFM--- 377
ACA4       317 TVGMRTEWGKLMETLVDGGEDETPLQVKLNGVATIIGKIGLSFAVLTFVVLCIRFVL--- 373
ACA11      317 TVGMRTEWGKLMDTLSEGGEDETPLQVKLNGVATIIGKIGLGFAVLTFVVLCIRFVV--- 373
ACA8       341 GVGVNTEWGLLMASISEDNGEETPLQVRLNGVATFIGSIGLAVAAAVLVILLTRYFTGHT 400
ACA9       354 GVGINTEWGLLMASISEDTGEETPLQVRLNGLATFIGIVGLSVALVVLVALLVRYFTGTT 413
ACA10      341 GVGVNTEWGLLMASVSEDNGGETPLQVRLNGVATFIGIVGLTVAGVVLFVLVVRYFTGHT 400
ACA12      313 SVGMSTTWGQTMSSINQDSSERTPLQVRLDTLTSTIGKIGLTVAALVLVVLLVRYFTGNT 372
ACA13      308 SVGMNTAWGQMMSHISRDTNEQTPLQSRLDKLTSSIGKVGLLVAFLVLLVLLIRYFTGTT 367
```

Fig.5 *Alignment of Arabidopsis ACA isoforms.*
A. N-terminal regulative region. Residues of the CaM-BD (*highlighted in blue*) and of the autoinhibitory domain (*underlined*) are identified in ACA8. **B.** Small cytoplasmic loop. Acidic residues of the stalk domain involved in pump autoinhibition (*highlighted in yellow*) shown to be conserved in cluster I, II and IV ACAs but variant in cluster III (*highlighted in green*), TM2 and TM3 are identified (underlined) in ACA12. Sequence alignment was performed using ClustalW.

Due to their distinctive features, cluster III ACA isoforms constitute, among their family, a notable exception, although poorly known. Indeed, while at least one isoform pertaining to clusters I, II and IV has been characterized, little was known so far on ACA12 and ACA13 [Boursiac and Harper, 2007; Bonza and De Michelis, 2011].

It has been shown that while the other ACAs are usually constitutively expressed, the transcript levels of ACA12 and ACA13 are almost undetectable; however their

expression appears to be dramatically increased by pathogens (such as *Botrytis cinerea* and *Pseudomonas siringae*) or UVB [Boursiac and Harper, 2007].

Taken together, these clues suggest that ACA12 and ACA13 may be required by the cell only under particular circumstances.

Aim of this work was therefore the study of the intracellular localization and the analysis of the activity and regulative properties of ACA12 (one members of cluster III), in order to investigate the physiological role for this pump.

Subcellular localization has been investigated by confocal microscopy in ACA12GFP-transformed *Arabidopsis thaliana* seedlings; instead the functional characterization has been performed in yeast *Saccharomyces cerevisiae*.

ACA12 was eterologously expressed in the *S. cerevisiae* strain K616, which is devoid of endogenous Ca^{2+} pumps (PMR1 and PMC1, respectively localized at the tonoplast and at the Golgi membrane) [Cunningham and Fink, 1994]. The K616 strain has been widely employed for the expression of heterologous Ca^{2+}-ATPases because they can be expressed, purified and characterized without the background activity from endogenous pumps [Sze et al., 2000]. In addition, this strain provides a good genetic complementation system for the *in vivo* study of the enzyme activity and regulative properties: indeed K616 is able to grow in a Ca^{2+}-depleted media only if it expresses a deregulated (fully active) Ca^{2+} pump [Curran et al., 2000; Bonza et al., 2004; Bækgaard et al., 2006]. Regulative properties of ACA12 (in both wild type and single point mutants forms) were tested *in vivo* for the ability to rescue the K616 phenotype in Ca^{2+}-depleted media. Moreover, yeast-expressed ACA12 was purified by CaM-affinity chromatography and its activity was studied *in vitro* measuring its Ca^{2+} and Ca^{2+}-CaM dependent ATP hydrolysis in order to unravel its biochemical properties.

Results

ACA12 localizes at the plasma membrane

The intracellular localization of ACA12 was established using Arabidopsis transgenic plants expressing GFP-fused ACA12 (ACA12-GFP) under the control of the 35S promoter (kindly provided by prof. J. F. Harper, University of Nevada, Reno). Seedlings were grown on plate, in the dark for 7-10 days; the root and the root tip (the last one is particularly suitable to distinguish the PM from the endomembranes due to the small vacuoles of the cells) were analyzed using a confocal microscope. The results summarized in **Fig. 6** (panels A, B, D, G) show that GFP fluorescence localizes at the periphery of the cells, compatibly with a PM localization of ACA12. In order to validate this result, the seedlings were also used to perform a co-localization of the GFP signal with the FM4-64 dye [Bolte et al., 2004] which is employed to mark the PM. The co-localization experiment gave positive results: fluorescence of GFP and FM4-64 clearly co-localize at the cell periphery (**Fig. 6**, panels D–I).

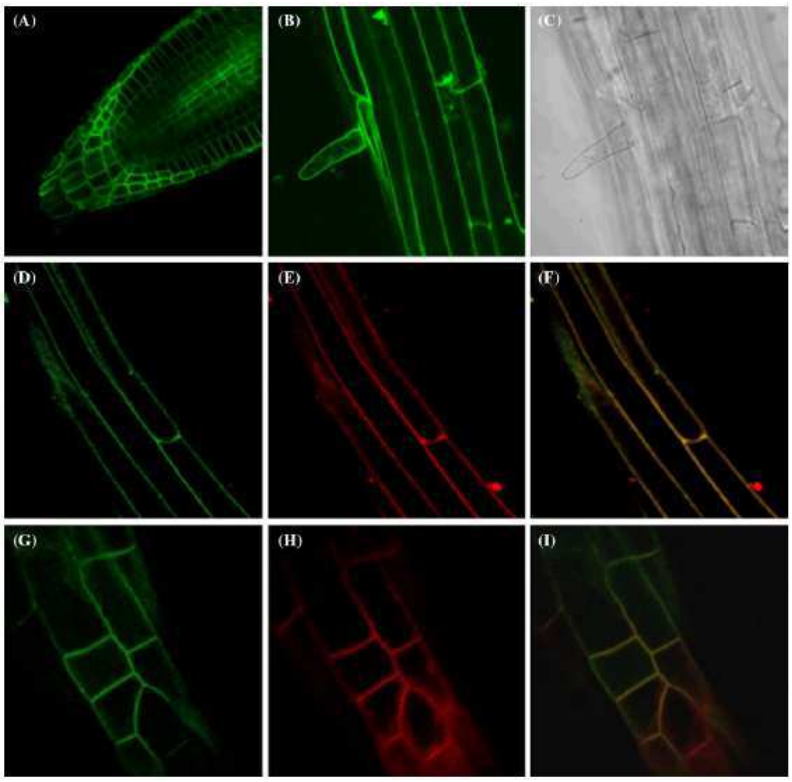

Fig.6 *ACA12-GFP is PM localized.*
Root images of 7–10 day old dark-grown seedlings expressing ACA12-GFP under the control of the 35S promoter. GFP fluorescence (A,B,D,G); phase contrast image of panel B (C); FM4-64 dye fluorescence (E,H); merging (F,I). Root tip (A); maturation root zone (B,C,D,E,F); elongation root zone (G,H,I).

Expression of ACA12 in yeast strain K616

ACA12-GFP (which contains also a C-terminal 6His tag) and ACA12 (without tags), cloned into the pYES2 vector under the control of the GAL1 promoter, were used to transform *Saccharomyces cerevisiae* strain K616. SDS-PAGE, Western blot and decoration with the HisProbe-HPR, which recognize the 6His tag fused to the C-terminal end of ACA12-GFP, were performed on the microsomal fraction of yeast expressing the tagged protein after standard induction conditions (24 h at 30 °C). The probe (**Fig. 7**) recognizes only a very faint band of the expected molecular mass (141 kDa); however several other band with lower molecular mass (likely due to protein proteolysis) are also identified. An increase in accumulation of the protein at the expected molecular weight was obtained lowering the temperature of the induction phase to 20 °C. Attempts to improve the ACA12-GFP expression yield by further lowering the induction temperature (18°C, 12°C) were unsuccessful (data not shown). However, also in the best condition (20°C), ACA12-GFP expression level remains very low with respect to a mutant form of the ACA8 isoform (the His-tagged Δ109-ACA8). In fact, the signal corresponding to Δ109-ACA8 is much stronger than that of ACA12-GFP, although 100 fold more microsomal proteins were loaded in the latter case.

ACA12 is functional and deregulated *in vivo*

Due to the lack of endogenous Ca^{2+}-ATPases, K616 yeast strain is unable to grow in Ca^{2+}-depleted media unless it expresses a deregulated form of ACA [Curran et al., 2000; Bonza et al., 2004; Baekgaard et al., 2006]. We therefore tested ACA12-GFP for its ability to rescue the phenotype of K616 at 20°C in a Ca^{2+}-depleted medium. The result (**Fig. 8**) shows that K616 yeast expressing ACA12-GFP is able to grow in a Ca^{2+}-depleted medium (in the presence of 5 mM EGTA) nearly as well as that expressing Δ74-ACA8, a deregulated ACA8 mutant. Conversely K616 expressing the WT form of ACA8 is unable to grow under these conditions [Bonza et al., 2004]. A rescue of K616 phenotype was also obtained by yeast transformation with the untagged ACA12. This result indicates that the yeast-expressed ACA12-GFP protein, as well as the ACA12 untagged protein, is functional and not auto-inhibited and that pump deregulation is not caused by the addition of the GFP at the C-terminal end of the protein.

Due to the relevant degree of proteolysis of ACA12-GFP (**Fig. 7**), and probably also of

ACA12, in yeast membrane, the possibility exists, albeit unlikely, that the rescue of K616 phenotype results from the presence of ACA12 fragments lacking the autoinhibitory domain rather than from a constitutive deregulation of ACA12. Therefore, in order to dismiss this possibility, we decided to purify ACA12 from yeast using CaM-affinity chromatography [Bonza et al. 1998, 2000; Fusca et al., 2009; Bonza and Luoni, 2010] and test its biochemical properties *in vitro*.

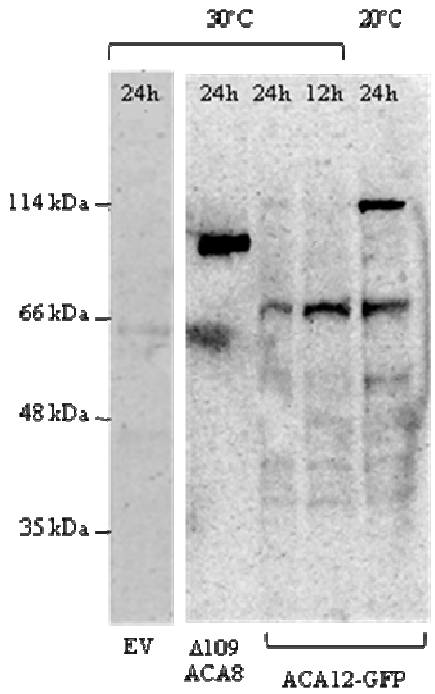

Fig.7 *Expression of ACA12-GFP in yeast strain K616.*
K616 yeast transformed with an empty *pYES2* vector (EV), with *Δ109-ACA8-6His* or with *ACA12-GFP* was grown in synthetic complete medium lacking uracil (SC-URA) supplemented with 2 % (w/v) glucose and 10 mM $CaCl_2$. To induce protein expression, the different yeast strains were grown at the specified temperatures for the indicated times in SC-URA medium containing 2 % (w/v) galactose, 1 % (w/v) raffinose and 10 mM $CaCl_2$. Solubilized microsomal proteins (30 µg for EV and ACA12-GFP and 0.3 µg for Δ109-ACA8) were subjected to SDS-PAGE, blotted and decorated with the HisProbe-HPR.

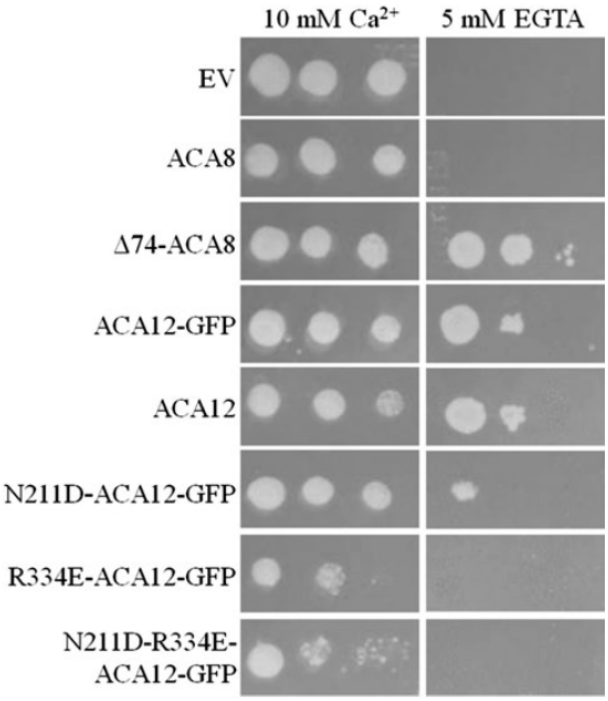

Fig.8 *Complementation test of the phenotype of K616 yeast strain.*
K616 yeast cells transformed with ACA12-GFP (WT and mutants) and ACA12 were grown in synthetic complete medium lacking uracil (SC-URA) and supplemented with 2 % (w/v) glucose and 10 mM $CaCl_2$. Cells were pelletted, washed and diluted with water to A_{600} = 1 - 0.3 -0.1. Five µL of each dilution were spotted on solid SC-URA medium containing 2 % (w/v) galactose and 1 % (w/v) raffinose, supplemented with 10 mM $CaCl_2$ or 5 mM EGTA. As controls, yeast strain K616 transformed with the *pYES2* empty vector (EV) or expressing full length ACA8 or the Δ74-ACA8 truncated mutant were used. Growth was recorded after 8 days of incubation at 20 °C. Results are from one experiment representative of three.

ACA12 is functional and deregulated *in vitro*

The microsomal proteins from K616 cells expressing ACA12-GFP were solubilized and incubated overnight with a CaM-Sepharose resin. After the removal of the unbound fraction, CaM-bound proteins were eluted upon Ca^{2+}-chelation with a 2 mM EGTA solution. The main fractions obtained from the purification procedure were subjected to SDS-PAGE, Western Blot and decoration with the HisProbe-HPR (**Fig. 9,** panel A, lane 1-3); otherwise following SDS-PAGE, proteins were labeled with the silver-stain method (**Fig. 9,** panel A, lane 4).

In the solubilized microsomal fraction (lane 1) the HisProbe-HPR recognizes the intact ACA12-GFP protein (141 kDa) and several other bands with lower molecular mass corresponding to His-tagged ACA12-GFP fragments. While these latter fragments are totally retained in the unbound fraction, a relevant portion of the intact ACA12-GFP

protein remains associated to the resin (lane 2). In the elution fraction only the 141 kDa band relative to the intact ACA12-GFP is recognized, while the His-tagged lower molecular weight bands are undetectable (lane 3). Moreover, in the EGTA-eluted fraction, the 141 kDa band is by far the most prominent after SDS-PAGE and silver staining (lane 4). These results indicate that CaM-affinity purification procedure allows the recovery of quite pure ACA12-GFP protein, albeit in tiny amounts (ca. 1 μg protein per mg of microsomal protein).

The same purification procedure was applied to microsomes from K616 cells expressing WT ACA12; purification fractions were subjected to SDS-PAGE and proteins were stained with comassie blue (**Fig. 9**, panel B). A band corresponding to ACA12 intact protein (113 kDa) is prominent in the EGTA-eluted fraction (lane 3), indicating that CaM-affinity also allows purification of the untagged ACA12 protein, albeit still with low yield (ca. 1 μg ACA12 per mg of microsomal protein).

Enzyme activity of the purified ACA12 protein was measured as Ca^{2+} dependent and Ca^{2+}-CaM dependent Mg^{2+}-ATP hydrolysis (**Table 1**). The purified ACA12 protein has Ca^{2+}-ATPase activity insensitive to CaM even when supplied at 10 μM concentration, but sensitive to vanadate, a well-known inhibitor of P-type ATPases. Instead ACA12 differs from the other ACAs characterized so far for being unable to use ITP as an alternative substrate to ATP [Bonza and De Michelis, 2011]. Moreover ACA12 is less sensitive to inhibition by eosin Y (**Fig. 10**), a fluorescein derivative which acts as a competitive inhibitor with respect to the nucleoside triphosphate substrate [De Michelis et al., 1993]. In fact eosin Y inhibit ACA12 activity at micromolar concentrations whereas nanomolar concentrations of the fluorescein derivative are sufficient to inhibit ACA8 [Bonza et al., 2004].

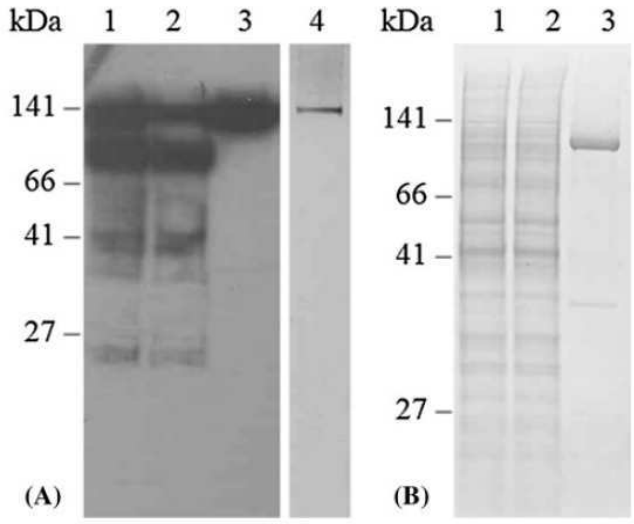

Fig.9 *Purification of ACA12-GFP and ACA12 by CaM-Sepharose affinity.*
Panel A (ACA12-GFP): *lane 1*, 10 µl of solubilized microsomal proteins (40 µg); *lane 2*, 10 µl of the unbound protein fraction; *lane 3*, 9 µl of the EGTA-eluted fraction; *lane 4*, 1 µl of the EGTA-eluted fraction concentrated ten-fold. Fractions were subjected to SDS-PAGE, blotted and decorated with the HisProbe-HPR (*lanes 1–3*) or silver-stained (*lane 4*). *Panel B (ACA12)*: *lane 1*, 10 µl of solubilized microsomal proteins (40 µg); *lane 2*, 10 µl of the unbound protein fraction; *lane 3*, 3.5 µl of the EGTA eluted fraction concentrated 20-fold. Fractions were subjected to SDS-PAGE and stained with Comassie blue.

Assay conditions	Ca^{2+}-ATPase activity (nmol Pi min^{-1} mg^{-1} protein)
ATP	289 ± 27
ATP + 1 µM CaM	303 ± 31
ATP + 10 µM CaM	309 ± 29
ATP + 200 µM vanadate	3 ± 1
ITP	25 ± 3

Table. 1 *Ca^{2+}-ATPase activity of ACA12*
The specific activity of ACA12 purified protein was measured, at the specified conditions, as Ca^{2+} dependent Mg^{2+}-ATP or Mg^{2+}-ITP hydrolysis. Results (plus or minus standard error of the mean) are from three experiments, each with three replicates, performed on different purified fractions.

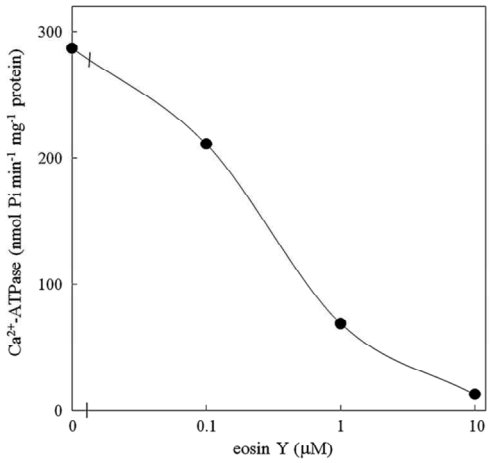

Fig.10 *Effect of eosin Y on ACA12 activity*
Effect of eosin Y on ACA12 activity was measured as Ca^{2+} dependent Mg^{2+}-ATP hydrolysis in the presence of the specified eosin Y concentrations. Results are from one experiment, representative of three.

ACA12 single point mutants lose the ability to rescue K616 phenotype

In studies on other ACA isoforms, as well as on a PMCA, two acidic residue (an Asp and a Glu) respectively localized at the edge of TM2 and of TM3 were found to be important for IIB P-type ATPases autoinhibition. Single point mutations of each of these acidic residues generates constitutively active proteins, insensitive to CaM [Curran et al., 2000; Bredeston and Adamo, 2004; Fusca et al., 2009]. Alignment of ACA12 (**Fig. 5**) with the other ACAs of Arabidopsis shows that these two residues, conserved in all members of the other three clusters, are variant in cluster III isoforms ACA12 and ACA13. In particular ACA12 Asn^{211} and Arg^{334} respectively align with the Asp and the Glu conserved in ACA isoforms belonging to the other three clusters. We generated ACA12-GFP single mutants harboring a $N^{211}D$ or a $R^{334}E$ substitution as well as the $N^{211}D$-$R^{334}E$ double mutant. All mutants, expressed in K616 at levels similar to that of the WT protein (data not shown), were tested for their ability to rescue K616 phenotype in a Ca^{2+}-depleted medium (**Fig. 8**). While the $N^{211}D$ mutation only partially impairs the ability of ACA12-GFP to rescue the growth phenotype, there was no rescue for K616 yeast expressing ACA12-GFP $R^{334}E$ or ACA12-GFP $N^{211}D$-$R^{334}E$ double mutant.

Discussion

Discussion

Subcellular localization experiments, performed on ACA12-GFP transformed Arabidopsis seedlings (**Fig. 6**), indicate that ACA12 is a plasma membrane protein which co-localizes with the PM dye FM4-64 [Bolte et al., 2004], as previously assumed by Frei dit Frey and colleagues [2012]. Further experiments also demonstrated that ACA12 is able to rescue the phenotype of an Arabidopsis knock-out mutant lacking ACA9 (a PM isoform primarily expressed in pollen [Schiøtt et al., 2004]), when expressed under the control of ACA9 promoter [Limonta et al., 2013]. This confirms the PM-localizion of ACA12, but also indicate that it is functional as Ca^{2+} pump in Arabidopsis.

The employment of *S. cerevisiae* strain K616 provides a powerful genetic complementation system for studying the functional and regulatory properties of ACA12. Indeed despite the low expression level of ACA12 in yeast membrane (**Fig. 7**), this pump is able to complement the K616 phenotype, making it able to grow in Ca^{2+} limiting conditions (in the presence of 5 mM EGTA) (**Fig. 8**), as other deregulated (fully active) mutants of ACA isoforms are able to do [Curran et al., 2000; Bonza et al., 2004; Baekgaard et al., 2006]. These data not only confirm the *in vivo* functionality of ACA12 as a Ca^{2+}-ATPase, but also indicate that ACA12 is a deregulated isoform of Arabidopsis type IIB Ca^{2+} pump.

In vitro biochemical assay of the activity of the purified ACA12 confirmed pump deregulation: ACA12 activity could not be stimulated by CaM (**Table 1**). With respect to the other ACA isoforms, ACA12 sequence is highly divergent in the regulatory N-terminus which contains the auto-inhibitory domain and the CaM-binding sites (**Fig. 5**): in particular only one of the two anchor residues in the high affinity CaM-binding site (Trp^{28} of ACA12) is conserved. However, ACA12 retains the ability to bind CaM, in fact it can be purified by CaM-affinity chromatography (**Fig. 9**). We supposed that the lack of ACA12 autoinhibition may be connected to the lack of two acidic residues, localized at the cytosolic edge of TM2 and TM3. These residues (an Asp and a Glu) are instead conserved in other clusters of ACAs as well as in the animal orthologue PMCA, their mutation inducing the deregulation of the pumps [Curran et al., 2000; Bredeston and Adamo, 2004; Fusca et al., 2009], seemingly not because of the interruption of the interaction between the autoinhibitory domain with its intramolecular target but due the change of the Ca^{2+} binding site accessibility [Bredeston and Adamo, 2004; Corradi and Adamo, 2007]. Alignment of ACA12 sequence with the other ACA isoforms pointed out

that the conserved Asp and Glu residues align respectively with Asn^{211} and Arg^{334} in ACA12 (**Fig. 5**). Reverting Asn^{211} to Asp and Arg^{334} to Glu in ACA12 sequence determines mutant pumps inability to complement the K616 phenotype (only partially for N211D alone, completely for R334E and N211D-R334E mutations, **Fig. 8**). These results, that must be taken as preliminary, seem to confirm the recovery of autoinhibition, but an alternative explanation exists: the activity of the purified R334E mutant was barely detectable even in the presence of CaM (data not shown), and if this can be due to a protein damage occurred during extraction, it is also possible that the mutation generated a non functional protein in first place.

A hint supporting protein instability during extraction is that, while ACA12 WT successfully complements the K616 phenotype despite its low expression level, after purification its activity is low compared to CaM-stimulated activity of ACA8 purified under the same conditions (unpublished data; [Bonza and Luoni, 2010]). Its fragility is further confirmed by a 50-80% activity decrease upon storage at -80 °C (data not shown): ACA12 activity could be preserved overnight only upon storage at 4 °C in the presence of phosphatidylcholine (100-fold molar excess). Moreover the expression of ACA12-GFP under the control of the 35S promoter in mature leaves of Arabidopsis is fairly low (data not shown).

ACA12 differs from the other ACAs characterized so far for being virtually unable to use ITP as a substrate alternative to ATP, and for being less sensitive to inhibition by the fluorescein derivative eosin Y (**Table 1**, **Fig. 10**). Since fluorescein and its derivatives are competitive inhibitors of P-type ATPases, which act by binding to a conserved Lys residue in the nucleotide-binding domain, these results suggest that the conformation of this domain in ACA12 is more similar to that of other P-type ATPase (which are ATP-specific and less sensitive to inhibition by fluorescein derivatives) than to that of ACA isoforms pertaining to the other three clusters [De Michelis et al., 1993; Bonza et al., 2004; Bonza and De Michelis, 2011].

The role of a deregulated ACA isoform as ACA12 within the physiology of the plant is still an open question. Unlike the relatively constant and redundant expression of other Arabidopsis ACAs, members of cluster III normally show very low or undetectable levels of expression under normal growth conditions. However, ACA12 and ACA13 are induced up to 40-fold in response to a pathogen stress (infection with *Botrytis cinerea* and *Pseudomonas syringae*) [Boursiac and Harper, 2007]. While it is not known why ACA12 and ACA13 show such dramatic profiling change, this may indicate a unique biochemical

activity that is required only under special circumstances. In particular ACA12 over-expression upon exposure to pathogens suggests that it may be involved in the adaptive response to these stress signals: expression of a deregulated PM Ca^{2+}-ATPase may impact on the shape of pathogen-induced Ca^{2+} transients [Boller and Felix, 2009; Ranf et al., 2011] and consequently on the response of the plant to a new pathogen attack. Moreover it has been seen that ACA13 espression level is up-regulated in mekk1-/- knock-out Arabidopsis plants. MEKK1 encodes a mitogen-activated protein kinase kinase kinase which acts as negative regulator of the pathogen response pathway activated by the interaction of the bacterial elicitor flagellin with its receptor (FLS2). The gene expression profile of MEKK1 knock-out plants matches with those of plant treated with *B. cinerea* and *P. syringae*, with disruption of the MEKK1 gene resulting in up-regulation of pathogenesis-associated genes [Suarez-Rodriguez et al., 2006].

The finding that, under normal conditions, ACA12 also shows significant levels of expression in guard cells [http://bar.utoronto.ca/efp_arabidopsis/cgibin/efpWeb .cgi; Winter et al., 2007] may provide an additional clue on its involvement in plant pathogen response. Stomata are indeed preferential entry points for pathogen invasion and undergo closure upon detection of bacterial elicitor to prevent infection [Schulze-Lefert and Robatzek, 2006]. It has been demonstrated that elicitor-induced transient increase in $[Ca^{2+}]_c$, which results in stomata closure, requires the availability of extracellular Ca^{2+} pool, according to studies showing that extracellular Ca^{2+} is necessary for the induction of plant defense responses against pathogen [Klüsener et al., 2002; Aslam et al., 2008]. In this context the expression of a deregulated PM-localized Ca^{2+}-ATPase, as ACA12, may provide a Ca^{2+} extrusion activity supporting Ca^{2+}-dependent plant pathogen defense.

Interestingly, when transiently expressed in *N. benthamiana* leaves, ACA12 (as ACA8) interacts at the PM with the brassinosteroid receptor BRI1 and with CLV1 [Frei dit Frey et al., 2012] and interactomic screening by the split ubiquitin test has identified four orphan receptor like kinases (RLKs) as specific ACA12 interactors [http://cas-biodb.cas.unt.edu/project/mind/search.php]. RLKs are members of a large family of kinases (more than 600 members in Arabidopsis) which are involved in diverse ligand-mediated signaling pathways. In particular several RLKs have been shown to be receptor proteins involved in perception of pathogens [Shiu and Bleecker, 2001Boller and Felix, 2009; Ranf et al., 2011; Gish and Clark, 2011]. We might speculate that the activity of ACA12 may be modulated by RLK phosphorylation in order to provide the optimal contribution to plant response to pathogen attack.

Finally, as previously reported for *Oryza sativa* by Baxter and collegues [2003], cluster III Arabidopsis isoforms show to be conserved also in other plant species. A phylogenetic comparison of protein sequences of Arabidopsis ACAs with putative IIB P-type ATPases pertaining to other species of agronomic interest (such as *Vitis vinifera*, *Solanum lycopersicum*, *Populus trichocarpa*, *Cucumis melo*, *Zea mays* and *Brachypodium distachyon*) revealed that at least one isoform for each species clusters together with ACA12 and ACA13 (**Fig. 11**). Moreover, sequence alignments showed that, ACA12 and ACA13 orthologues also show amino acidic variations of the conserved Asp and Glu residues involved in determining ACAs autoinhibition (data not shown), therefore suggesting a cluster-specific activity regulation conserved among different plant species. Cluster III conservation in various plant species may be an additional clue of the physiological relevance of these isoforms.

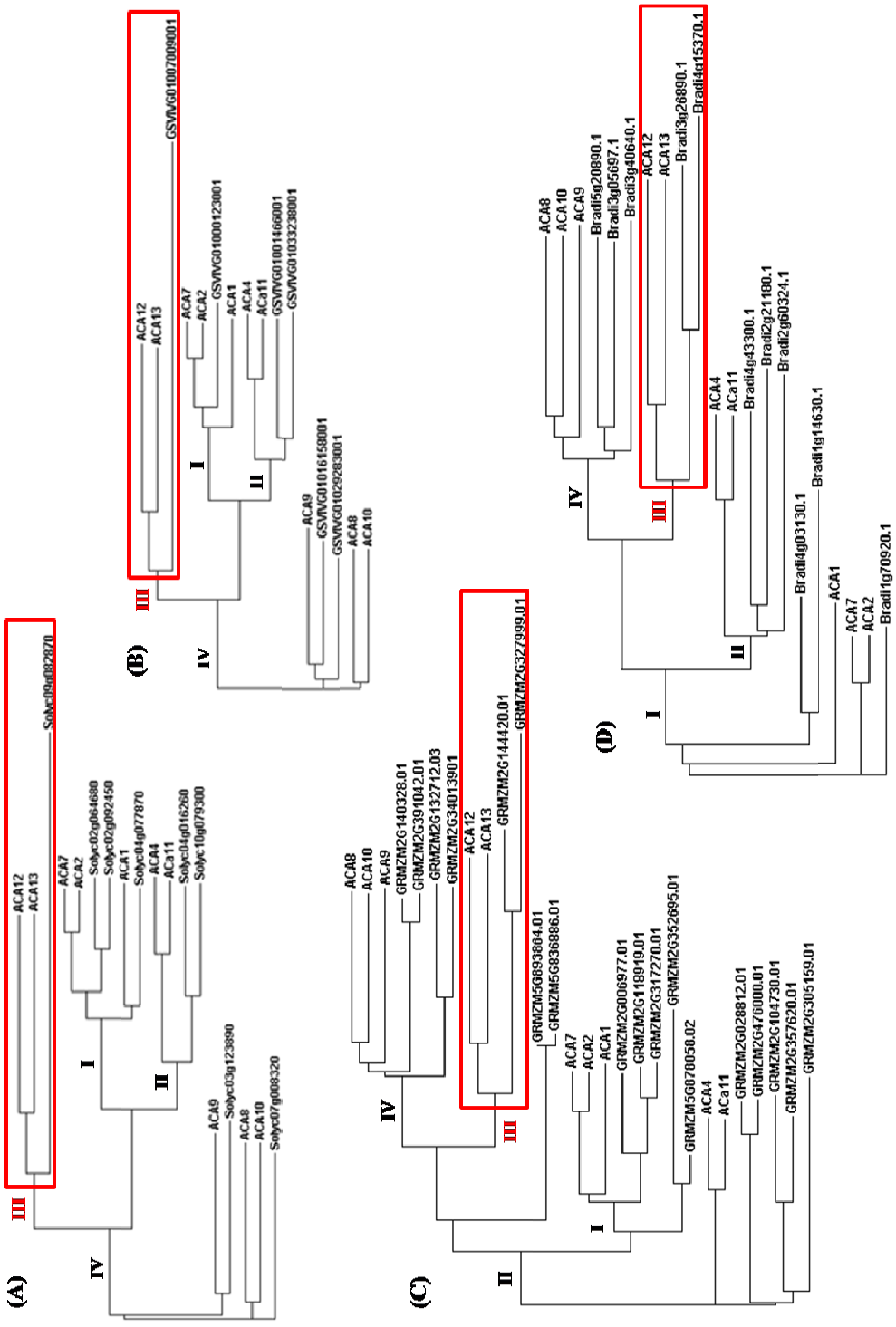

Fig.11 *Phylogenetic trees of IIB P-type ATPases.*
Protein sequences of putative IIB ATPases from *Solanum lycopersicum* (A),*Vitis vinifera* (B), *Zea mays* (C) and *Brachypodium distachyon* (D) were aligned with sequence of ACA members of *Arabidopsis thaliana* using ClustalW2 Multiple Sequence Alignment. Phylogenetic tree were constructed from full-length protein sequences with the neighbor joining method (NJ) using ClustalW2. Numbers (I, II, III, IV) denote clusters. Cluster III members are boxed in red.

References

References

Anil VS, Rjkumar P, Kumar P, Mathew MK (2008) A plant Ca^{2+} pump, ACA2, relieves salt hypersensitivity in yeast. Modulation of cytosolic calcium signature and activation of adaptive Na^{+} homeostasis. Journal of Biological Chemistry. **283**: 3497-3506.

Aslam SN, Newman MA, Erbs G, Morrissey KL, Chinchilla D, Boller T, Jensen TT, De Castro C, Ierano T, Molinaro A, Jackson RW, Knight MR, Cooper RM (2008) Bacterial polysaccharides suppress induced innate immunity by calcium chelation. Current Biology. **18**:1078-83.

Axelsen KB, Palmgren MG (1998) Evolution of substrate specificities in the P-type ATPases superfamily. Journal of Molecular Evolution. **46**:84-101.

Axelsen KB, Palmgren MG (2001) Inventory of the superfamily of P-type ion pumps in Arabidopsis. Plant Physiology **126**:696-706.

Bækgaard L, Luoni L, De Michelis MI and Palmgren MG (2006) The plant plasma membrane Ca^{2+} pump ACA8 contains overlapping as well as physically separated autoinhibitory and calmodulin-binding domains. Journal of Biological Chemistry. **281**:1058-1065.

Baxter I, Tchieu J, Sussman MR, Boutry M, Palmgren MG, Gribskov M, Harper JF and Axelsen KB (2003) Genomic comparison of P-type ATPase ion pumps in *Arabidopsis* and rice. Plant Physiology. **132**: 618-628.

Beffagna N, Romani G and Sforza MC (2000) H^{+} fluxes at plasmalemma level: in vivo evidences for a significant contribution of the Ca^{2+}-ATPase and for the involvement of its activity in the abscisic acid-induced changes in *Egeria densa* leaves. Plant Biology. **2**: 168- 175.

Boller T, Felix G (2009) A renaissance of elicitors: perception of microbe associated molecular patterns and danger signals by pattern-recognition receptors. Annual Review of Plant Biology. **60**: 379-406.

Bolte S, Talbot C, Boutte Y, Catrice O, Read ND, Satiat-Jeunemaitre B (2004) FM-dyes as experimental probes for dissecting vesicle trafficking in living plant cells. Journal of Microscopy. **214**:159–173.

Bonza MC, Carnelli A, De Michelis MI, Rasi-Caldogno F (1998) Purification of the plasma membrane Ca^{2+}-ATPase from radish seedlings by calmodulin-agarose affinity chromatography. Plant Physiology. **116**:845–851.

Bonza MC, De Michelis MI (2011) The plant Ca^{2+}-ATPase repertoire: biochemical features and physiological functions. Plant Biology; **13**: 421–430.

Bonza MC, Luoni L (2010) Plant and animal type 2B Ca^{2+}-ATPases: evidence for a common auto-inhibitory mechanism. FEBS Letters. **584**:4783-8.

Bonza MC, Luoni L, De Michelis MI (2001) Stimulation of plant plasma membrane Ca^{2+}-ATPase activity by acidic phospholipids. Physiologia Plantarum. **112**:315–320.

Bonza MC, Luoni L, De Michelis MI (2004) Functional expression in yeast of an N-deleted form of At-ACA8, a plasma membrane Ca^{2+}-ATPase of *Arabidopsis thaliana*, and characterization of a Hyperactive mutant. Planta. **218**: 814-823.

Bonza MC, Morandini P, Luoni L, Geisler M, Palmgren MG, De Michelis MI (2000) *At*-ACA8 encodes a plasma membrane-localized calcium-ATPase of *Arabidopsis* with a calmodulin-binding domain at the N-terminus. Plant Physiology. **123**: 1495-1505.

Bonza MC, Loro G, Behera S, Wong A, Kudla J, Costa A (2013) Analyses of Ca^{2+} accumulation and dynamics in the endoplasmic reticulum of Arabidopsis root cells using a genetically encoded Cameleon sensor. Plant Physiology. **163**:1230-41.

Bose J, Pottosin II, Shabala SS, Palmgren MG, Shabala S (2011) Calcium efflux systems in stress signalling and adaptation in plants. Frontiers in Plant Science. **2**:1-12

Boursiac Y, Harper JF (2007) The origin and function of calmodulin regulated Ca^{2+} pumps in plants. Journal of Bioenergetic and Biomembranes. **39**: 409-414.

Boursiac Y, Lee SM, Romanowsky S, Blank R, Sladek C, Chung WS, Harper JF (2010) Disruption of the vacuolar calcium-ATPases in *Arabidopsis* results in the activation of a salicylic acid-dependent programmed cell death pathway. Plant Physiology. **154**:1158–1171.

Bredeston LM, Adamo HP (2004) Loss of autoinhibition of the plasma membrane Ca^{2+} pump by substitution of aspartic 170 by asparagin. Activation of plasma membrane calcium ATPase 4 without disruption of the interaction between the catalytic core and the C-terminal regulatory domain. Journal of Biological Chemistry. **279**:41619–41625.

Brini M, Carafoli E (2009) Calcium pumps in health and disease. Physiological Review. **89**:1341-1378.

Bublitz M, Morth JP, Nissen P (2011) P-type ATPases at a glance. Journal of Cell Science. **124**:2515-2519.

Bublitz M, Poulsen H, Morth JP, Nissen P (2010) In and out of the cation pumps: P-type ATPase structure revisited. Current Opinion in Structural Biology. **20**:431-9.

Cerana M, Bonza MC, Harris R, Sanders D, De Michelis MI (2006) Abscisic acid stimulates the expression of two isoforms of plasma membrane Ca^{2+}-ATPase in *Arabidopsis thaliana* seedlings. Plant Biology; **8**: 572-578.

Chourasia M, Sastry GN (2012) The Nucleotide, Inhibitor, and Cation Binding Sites of P-type II ATPases. Chemical Biology and Drug Design. **79**:617–627.

Corradi GR, Adamo HP (2007) Intramolecular fluorescence resonance energy transfer between fused autofluorescent proteins reveals rearrangements of the N- and C-terminal

segments of the plasma membrane Ca^{2+} pump involved in the activation. Journal of Biological Chemistry. **282**:35440-8.

Cunningham KW, Fink GR (1994) Calcineurin-dependent growth control in *Saccharomyces cerevisiae* mutant lacking PMC1, a homolog of plasma membrane Ca^{2+}-ATPases. Journal of Cell Biology. **124**: 351-363.

Curran AC, Hwang I, Corbin J, Martinez S, Rayle D, Sze H, Harper JF (2000) Autoinhibition of a calmodulin-dependent calcium pump involves a structure in the stalk that connects the transmembrane domain to the ATPase catalytic domain. Journal of Biological Chemistry. **275**:30301–30308.

De Falco TA, Bender KW and Snedden WA (2010) Breaking the code: Ca^{2+} sensors in plant signalling. Biochemical Journal. **425**:27-40.

De Michelis MI, Carnelli A, Rasi-Caldogno, F (1993) The Ca^{2+} pump of the plasma membrane of *Arabidopsis thaliana*: characteristics and sensitivity to fluorescein derivatives. Botanical Acta. **106**: 20-25.

Dodd AN, Kudla J, Sanders D (2010) The language of calcium signaling. Annual Review of Plant Biology. **61**:593–620.

Evans NH, McAinsh MR, Hetherington AM (2001) Calcium oscillations in higher plants. Current Opinion in Plant Biology. **4**:415-20.

Frei dit Frey N, Mbengue M, Kwaaitaal M, Nitsch L, Altenbach D, Häweker H, Lozano-Duran R, Njo MF, Beeckman T, Huettel B, Borst JW, Panstruga R, Robatzek S (2012) Plasma membrane calcium ATPases are important components of receptor-mediated signaling in plant immune responses and development. Plant Physiology. **159**:798–809.

Fusca T, Bonza MC, Luoni L, Meneghelli S, Marrano C, De Michelis MI (2009) Single point mutations in the small cytoplasmic loop of ACA8, a plasma membrane Ca^{2+}-ATPase of *Arabidopsis thaliana*, generate partially deregulated pumps. Journal of Biological Chemistry. **284**: 30881-30888.

Geisler M, Axelsen K, Harper JF, Palmgren MG (2000a) Molecular aspects of higher plant P-type Ca^{2+}-ATPases. Biochimical and Biophisical Acta. **1465**: 52-78.

Geisler M, Frangne N, Malmström S, Gomès E, Smith JAC, Martinoia E, Palmgren MG (2000b) The ACA4 gene of Arabidopsis encodes a vacuolar calcium pump that is involved in calcium signalling upon salt stress. Plant Physiology **124**: 1814-1827.

George L, Romanowsky SM, Harper JF, Sharrok RA (2008) The ACA10 Ca^{2+}-ATPase regulates adult vegetative development and inflorescence architecture in Arabidopsis. Plant Physiology **146**: 716-728.

Giacometti S, Marrano CA, Bonza MC, Luoni L, Limonta M, De Michelis MI (2012) Phosphorylation of serine residues in the N-terminus modulates the activity of ACA8, a

plasma membrane Ca^{2+}-ATPase of *Arabidopsis thaliana*. Journal of Experimental Botany. **63**:1215–1224.

Gish LA, Clark SE (2011) The RLK/Pelle family of kinases. Plant Journal. **66**:117–127.

Hepler PK (2005) Calcium: a central regulator of plant growth and development. The Plant Cell. **17**: 2142–2155.

Hetherington AM, Brownlee C (2004) The generation of Ca^{2+} signals in plants. Annual Review of Plant Biology. **55**:401-27.

Hirschi KD (2004) The calcium conundrum. Both versatile nutrient and specific signal. Plant Physiology. **136**:2438–2442.

Hwang I, Sze H and Harper JF (2000) A calcium-dependent protein kinase can inhibit a calmodulin-stimulated Ca^{2+} pump (ACA2) located in the endoplasmic reticulum of *Arabidopsis*. Proceedings of the National Academy of Science USA. **97**: 6224–6229.

James P, Vorherr T, Carafoli E (1995) Calmodulin-binding domains: just two faced or multi-faceted? Trends in Biochemical Science. **20**:38-42.

Jammes F, Hu HC, Villiers F, Bouten R, Kwak JM (2012) Calcium-permeable channels in plant cells. FEBS Journal. **278**:4262-4276.

Kabala K, Klobus G (2005) Plant Ca^{2+}-ATPases. Acta Physiologiae Plantarum. **27**:559–574.

Kamrul Huda KM, Yadav S, Akhter Banu MS, Trivedi DK, Tuteja N (2013) Genome-wide analysis of plant-type II Ca^{2+}-ATPases gene family from rice and Arabidopsis: potential role in abiotic stresses. Plant Physiology and Biochemistry. **65**:32-47.

Klüsener B, Young JJ, Murata Y, Allen GJ, Mori IC, Hugouvieux V, Schroeder JI (2002) Convergence of calcium signaling pathways of pathogenic elicitors and abscisic acid in Arabidopsis guard cells. Plant Physiology. **130**:2152-63.

Kudla J, Batistič O, Hashimoto K (2010) Calcium signals: the lead currency of plant information processing. Plant Cell. **22**: 541-63.

Kuhlbrandt W (2004) Biology, Structure and Mechanism of P-type ATPases. Molecular and Cellular Biology. **5**: 282-295.

Li X, Chanroj S, Wu Z, Romanowsky SM, Harper JF, Sze H (2008) A distinct endosomal Ca^{2+}/Mn^{2+} pump affects root growth through the secretory process. Plant Physiology. **147**: 1675–1689.

Limonta M, Romanowsky S, Olivari C, Bonza MC, Luoni L, Rosenberg A, Harper JF, De Michelis MI (2013) ACA12 is a deregulated isoform of plasma membrane Ca^{2+}-ATPase of Arabidopsis thaliana. Plant Molecular Biology.

Lucca N, Léon G (2012) *Arabidopsis* ACA7, encoding a putative auto-regulated Ca^{2+}-ATPase, is required for normal pollen development. Plant Cell Reports. **31**:651-659.

Luoni L, Meneghelli S, Bonza MC, De Michelis MI (2004) Auto-inhibition of *Arabidopsis thaliana* plasma membrane Ca^{2+}-ATPase involves an interaction of the N-terminus with the small cytoplasmic loop. FEBS Letters. **574**: 20-24.

Malmström S, Akerlund HE, Askerlund P (2000) Regulatory role of the N terminus of the vacuolar calcium-ATPase in cauliflower. Plant Physiology. **122**: 517-526.

Manohar M, Shigaki T, Hirschi KD (2011) Plant cation/H^+ exchangers (CAXs): biological functions and genetic manipulations. Plant Biology. **13**:561-569.

McAinsh MR and Pittman JK (2009) Shaping the calcium signature. New Phytology. **181**: 275-294.

Meneghelli S, Fusca T, Luoni L, De Michelis MI (2008) Dual mechanism of activation of plant plasma membrane Ca^{2+}-ATPase by acidic phospholipids: evidence for a phospholipid binding site which overlaps the calmodulin-binding site. Molecular Membrane Biology. **25**:539-46.

Møller JV, Olesen C, Lund Jensen AM, Nissen P (2005) The structural basis for coupling of Ca^{2+} transport to ATP hydrolysis by the sarcoplasmic reticulum Ca^{2+}-ATPase. Journal of Bioenergetics and Biomembranes. **37**:359-364.

Niggli V, Sigel E (2008) Anticipating antiport in P-type ATPases. Trends in Biochemical Sciences. **33**:156-160.

Palmgren MG, Axelsen KB (1998) Evolution of P-type ATPases. Biochimical and Biophysical Acta. **1365**:37-45.

Palmgren MG, Nissen P (2011) P-type ATPases. Annual Review of Biophysics. **40**: 243-266.

Pedersen CN, Axelsen KB, Harper JF, Palmgren MG (2012) Evolution of plant p-type ATPases. Frontiers in Plant Science. 3:31.

Pittman JK, Bonza MC and De Michelis MI (2010) Ca^{2+} pumps and Ca^{2+} antiporters in plant development. In: **M. Geisler & K. Venema (Eds).** *Transporters and pumps in plant signalling*. Springer-Verlag, Berlin, Heidelberg, D.

Ranf S, Eschen-Lippold L, Pecher P, Lee J, Scheel D (2011) Interplay between calcium signalling and early signalling elements during defence responses to microbe- or damage-associated molecular patterns. Plant Journal. **68**:100–113.

Rasi-Caldogno F, Carnelli A, De Michelis MI (1993) Controlled Proteolysis Activates the Plasma Membrane Ca^{2+} Pump of Higher Plants (A Comparison with the Effect of Calmodulin in Plasma Membrane from Radish Seedlings). Plant Physiology. **103**:385-390.

Romani G, Bonza MC, Filippini I, Cerana M, Beffagna N and De Michelis MI (2004) Involvement of the plasma membrane Ca^{2+}-ATPase in the short term response of *Arabidopsis thaliana* cultured cells to oligogalacturonides. Plant Biology. **6**:192-200.

Rudd JJ, Franklin-Tong VE (2001) Unravelling response-specificity in Ca^{2+} signaling pathways in plant cells. New Phytologist. **151**:7-33.

Sanders D, Brownlee C and Harper JF (1999) Communicating with calcium. Plant Cell. **11**:691-706.

Sanders D, Pelloux J, Brownlee C and Harper JF (2002) Calcium at the crossroads of signaling. Plant Cell. Supplement. 401-417.

Schiøtt M, Palmgren MG (2005) Two plant Ca^{2+} pump expressed in stomatal guard cells show opposite expression patterns during cold stress. Physiologia Plantarum. **124**: 278-283.

Schiøtt M, Romanowsky SM, Bækgaard L, Jakobsen MK, Palmgren MG, Harper JF (2004) A plant plasma membrane Ca^{2+} pump is required for normal pollen tube growth and fertilization. Proceedings of the National Academy of Science. **101**: 9502-9507.

Schulze-Lefert P, Robatzek S (2006) Plant pathogens trick guard cells into opening the gates. Cell. **126**:831-4.

Shigaki T, Hirschi KD (2006) Diverse Functions and Molecular Properties Emerging for CAX Cation/H^+ Exchangers in Plants. Plant Biology. **8**:419-429.

Shiu SH, Bleecker AB (2001) Receptor-like kinases from *Arabidopsis* form a monophyletic gene family related to animal receptor kinases. Proceedings of the National Academy of Science USA. **98**:10763–10768.

Spalding EP, Harper JF (2011) The ins and outs of cellular Ca^{2+} transport. Current Opininion in Plant Biology. **14**:715-20.

Stael S, Wurzinger B, Mair A, Mehlmer N, Vothknecht UC, Teige M (2012) Plant organellar calcium signalling: an emerging field. Journal of Experimental Botany. **63**:1525-1542.

Suarez-Rodriguez MC, Adams-Phillips L, Liu Y, Wang H, Su SH, Jester PJ, Zhang S, Bent AF, Krysan PJ (2006) MEKK1 is required for flg22-induced MPK4 activation in Arabidopsis plants. Plant Physiology. **143**:661-9.

Sze H, Liang F, Hwang I, Curran AC, Harper JF (2000) Diversity and regulation of plant Ca^{2+} pumps: insights from expression in yeast. Annual Review of Plant Physiology. Plant Molecular Biology. **51**: 433-462.

Tidow H, Poulsen LR, Andreeva A, Knudsen M, Hein KL, Wiuf C, Palmgren MG, Nissen P (2012) A bimodular mechanism of calcium control in eukaryotes. Nature. **491**:468–472.

Toyoshima C, Nomura H, Sugita Y (2003) Structural basis of ion pumping by Ca^{2+}-ATPase of sarcoplasmic reticulum. FEBS Letters. **555**:106-110.

Toyoshima C, Inesi G (2004) Structural basis of ion pumping by Ca^{2+}-ATPase of the sarcoplasmic reticulum. Annual Review of Biochemestry. **73**: 269-92.

Winter D, Vinegar B, Nahal H, Ammar R, Wilson GV, Provart NJ (2007) An "electronic fluorescent pictograph" browser for exploring and analyzing large-scale biological data sets. PLoS ONE. **2**:e718.

White PJ and Broadley MR (2003) Calcium in plants. Annals of Botany. **92**: 487-511.

Wu Z, Liang F, Hong B, Young JC, Sussman MR, Harper JF and Sze H (2002) An Endoplasmic Reticulum-Bound Ca^{2+}/Mn^{2+} Pump, ECA1, Supports Plant Growth and Confers Tolerance to Mn^{2+} Stress. Plant Physiology. **130**: 128-137.

Zielinski RE (1998) Calmodulin and calmodulin-binding proteins in plants. Annual Review of Plant Physiology and Plant Molecular Biology. **49**: 697-725.

Part II

Publication

Limonta M, Romanowsky S, Olivari C, Bonza MC, Luoni L, Rosemberg A, Harper JF, De Michelis MI (2013) Plant Molecular Biology. Epub ahead of print.

ACA12 is a deregulated isoform of plasma membrane Ca^{2+}-ATPase of *Arabidopsis thaliana.*

Plant Mol Biol
DOI 10.1007/s11103-013-0138-9

ACA12 is a deregulated isoform of plasma membrane Ca^{2+}-ATPase of *Arabidopsis thaliana*

Margherita Limonta · Shawn Romanowsky · Claudio Olivari · Maria Cristina Bonza · Laura Luoni · Alexa Rosenberg · Jeffrey F. Harper · Maria Ida De Michelis

Received: 7 June 2013 / Accepted: 29 September 2013

Abstract Plant auto-inhibited Ca^{2+}-ATPases (ACA) are crucial in defining the shape of calcium transients and therefore in eliciting plant responses to various stimuli. *Arabidopsis thaliana* genome encodes ten ACA isoforms that can be divided into four clusters based on gene structure and sequence homology. While isoforms from clusters 1, 2 and 4 have been characterized, virtually nothing is known about members of cluster 3 (ACA12 and ACA13). Here we show that a GFP-tagged ACA12 localizes at the plasma membrane and that expression of ACA12 rescues the phenotype of partial male sterility of a null mutant of the plasma membrane isoform ACA9, thus providing genetic evidence that ACA12 is a functional plasma membrane-resident Ca^{2+}-ATPase. By ACA12 expression in yeast and purification by CaM-affinity chromatography, we show that, unlike other ACAs, the activity of ACA12 is not stimulated by CaM. Moreover, full length ACA12 is able to rescue a yeast mutant deficient in calcium pumps. Analysis of single point ACA12 mutants suggests that ACA12 loss of auto-inhibition can be ascribed to the lack of two acidic residues—highly conserved in other ACA isoforms—localized at the cytoplasmic edge of the second and third transmembrane segments. Together, these results support a model in which the calcium pump activity of ACA12 is primarily regulated by increasing or decreasing mRNA expression and/or protein translation and degradation.

Keywords Ca^{2+}-ATPase · Plasma membrane · Calmodulin · *Arabidopsis thaliana*

Electronic supplementary material The online version of this article (doi:10.1007/s11103-013-0138-9) contains supplementary material, which is available to authorized users.

M. Limonta · C. Olivari · M. C. Bonza · L. Luoni · M. I. De Michelis (✉)
Dipartimento di Bioscienze, Istituto di Biofisica del CNR, Sezione di Milano, Università degli Studi di Milano, via G. Celoria 26, 20133 Milan, Italy
e-mail: mariaida.demichelis@unimi.it

S. Romanowsky · A. Rosenberg · J. F. Harper
Biochemistry Department, University of Nevada, Reno, NV 89557, USA

Present Address:
S. Romanowsky
Lilly Biotechnology Center-San Diego, 10300 Campus Point Drive, Suite 200 (East Lobby), San Diego, CA 92121, USA

Introduction

Plant sensing of different environmental stimuli such as cold, light, osmotic, salt and drought signals, oxidative stress, plant hormones and pathogens, activate signal transduction systems involving transient increases in cytosolic free Ca^{2+} concentration. The specificity of the response to the various environmental changes depends on the amplitude, frequency and localization of the cytosolic calcium transient. Transient increases in cytosolic Ca^{2+} are triggered by the opening of Ca^{2+} permeable channels that mediate passive ion influx from the apoplast and/or intracellular compartments, while Ca^{2+} active transporters (Ca^{2+}-H^{+} antiporters and Ca^{2+}-ATPases) determine the recovery of the resting cytosolic free Ca^{2+} concentration after the stimulus. Ca^{2+}-ATPases are thought to be crucial in defining the shape of the calcium transient and therefore in eliciting plant specific response to various stimuli (Sanders et al. 2002; McAinsh and Pittman 2009; Dodd et al. 2010; Kudla et al. 2010; Pittman et al. 2011; Spalding and Harper 2011; Bose et al. 2011).

Published online: 08 October 2013

Plant Ca^{2+}-ATPases belong—as those of animals—to subgroup 2 of P-type ATPases super-family, which are characterized by forming a phosphorylated intermediate which changes conformation during the catalytic cycle, and by a number of highly conserved sequence motifs (Møller et al. 1996; Axelsen and Palmgren 1998; Palmgren and Nissen 2011). The genome of higher plants encodes several Ca^{2+}-ATPases which group either with animal sarco-endoplasmic reticulum Ca^{2+}-ATPase in the 2A subgroup of P-type ATPases (ECA, ER-type Ca^{2+}-ATPase) or with animal plasma membrane (PM) Ca^{2+}-ATPase in the 2B subgroup (ACA, auto-inhibited Ca^{2+}-ATPase). Arabidopsis (*Arabidopsis thaliana*) has four ECA and ten ACA genes, with most cells expressing multiple isoforms (Geisler et al. 2000a; Sze et al. 2000; Bonza and De Michelis 2011; Pedersen et al. 2012).

A distinctive feature of ACAs in comparison to ECAs is an extended cytosolic N-terminal domain. In previously characterized members of the ACA subgroup, the N-terminus has been found to have an auto-inhibitory domain and a partially overlapping high affinity calmodulin (CaM) binding site (Geisler et al. 2000a; Baxter et al. 2003; Kabala and Klobus 2005; Boursiac and Harper 2007; Bonza and De Michelis 2011; Pedersen et al. 2012); a second low affinity CaM-binding site has been recently identified just 8 aa downstream the first one in ACA8, one of the best characterized ACA isoform (Tidow et al. 2012). In all ACA isoforms characterized so far, CaM-binding suppresses the auto-inhibitory action of the N-terminus, increasing V_{max} and decreasing $K_{0.5}$ for free Ca^{2+}.

ACA isoforms can be divided into 4 clusters, based on sequence alignments and intron number and/or position (Baxter et al. 2003): the current evidence suggests that each cluster harbors isoforms with different features, such as sub-cellular localization or regulatory mechanisms (Baxter et al. 2003; Bonza and De Michelis 2011). The abundance of ACA isoforms, together with their co-expression in the same cell types, makes it difficult to define the role of each isoform in the physiology of the plant: however the phenotype of knock out mutants provides evidence for their role in development and/or response to biotic and abiotic stresses (Schiøtt et al. 2004; George et al. 2008; Boursiac et al. 2010; Frei dit Frey et al. 2012). Gaining a deeper knowledge on the biochemical properties and regulation of different ACA isoforms is important to assign them specific functions in vivo and therefore in understanding the biochemical pathways associated to relevant plant responses.

While at least one ACA has been previously characterized from clusters 1, 2 and 4, virtually nothing is known about members of cluster 3, which in Arabidopsis are isoforms ACA12 and ACA13. These isoforms, which are unique in being encoded by intron-less genes, have very low expression level in most cell types under basal conditions, but are dramatically induced upon exposure to a specific stress, such as in response to pathogens or UVB stress [(Boursiac and Harper 2007); http://bar.utoronto.ca/efp_arabidopsis/cgi-bin/efpWeb.cgi (Winter et al. 2007)]. Their N-terminal regions are highly divergent compared to those of other ACAs; moreover they have an Asn (N211 in ACA12) and an Arg (R334 in ACA12) at positions close to transmembrane domain (TM) 2 and 3 respectively, where all other ACAs—as well as animal PM Ca^{2+}-ATPases—have an acidic residue. In different ACA isoforms, as well as in an animal pump isoform, mutation of these acidic residues generates deregulated pumps that show near full activity without further activation by CaM (Curran et al. 2000; Bredeston and Adamo 2004; Fusca et al. 2009).

Here we provide genetic evidence that ACA12 is a functional PM-resident Ca^{2+}-ATPase, and biochemical evidence that ACA12 binds CaM but, unlike other ACAs, is not stimulated by CaM. In addition, a full length ACA12 is able to rescue a yeast mutant deficient in calcium pumps, unlike other well studied ACAs such as ACA8, which only provides a rescue when its auto-inhibitory N-terminus is deleted (Bonza et al. 2004; Baekgaard et al. 2006). Together, this supports a model in which the calcium pump activity provided by ACA12 is not dependent on Ca^{2+}-CaM stimulation, would be therefore primarily regulated by increasing or decreasing mRNA expression and/or protein translation and degradation.

Materials and methods

Plant lines and growth conditions

Arabidopsis thaliana ecotypes WS or Columbia were used for all plant experiments. For testing the ability of an *ACA12* (At3g63380) gene to rescue a loss of function of *ACA9* (At3g21180), two WS ecotype-based *T-DNA* insertion alleles were used, *aca9-1* and *aca9-2* (Schiøtt et al. 2004). For subcellular localization experiments, a transgene encoding an ACA12-GFP was transformed into *A. thaliana* ecotype Columbia.

For growing plants, seeds were sown on 0.5× Murashige and Skoog (MS) medium, pH 5.7 and stratified at 4 °C for 48 h. Seedlings were grown at room temperature (22 °C) under 24 h light for 7–10 days before being transplanted to soil. The soil used was Sunshine SMB-238 supplemented with 10-10-10 fertilizer (Hummert) and Marathon pesticide (Hummert) following the manufacturer's instructions. Plants were grown until maturity in a green house (with light and temperature conditions varying by seasons), or in growth chambers with a photoperiod of 16 h of light at 20 °C and 8 h of dark at 18 °C.

Plasmid construction

Plasmid construct *35S::ACA12-GFP* (plasmid stock ps 391, see Online Resource 1), encodes an ACA12 with a C-terminal GFP followed by a 6His tag, downstream of a 35S promoter in a *pBIN101.2* plant expression vector (Bevan 1984), harboring a kanamycin (kan^r) resistance marker for bacterial and plant selections. This *ACA12* coding sequence was generated by PCR amplification of genomic DNA from *A. thaliana* (Columbia), and sub-cloning into a *pBIN101.2* plant expression vector (Bevan 1984). The *ACA12* coding sequence begins with ATGAGGGACCTC and ends with CTCAAGAAACCT. The stop codon was removed to allow an in frame fusion with a GFP. The genomic sequence for *ACA12* does not contain any intron. The absence of PCR mistakes was confirmed by DNA sequencing.

Plasmid construct *ACA9promoter::ACA12-TAP2(YFP)* (ps 688, see Online Resource 1), encodes an ACA12 with a C-terminal YFP downstream of a promoter from a preferentially pollen expressed gene, *ACA9* (Schiøtt et al. 2004). This construct was based on a derivative of the *pGreenII* plant expression vector (Hellens et al. 2000) [kan^r in bacteria, hygromycin-resistance (hyg^r) in plants]. Plasmid construct *ACA9promoter::ACA2-TAP2(GFP)* (ps 585, see Online Resource 1), is similar to ps 688 except that it encodes an ER-localized ACA2 (Hong et al. 1999) fused to GFP.

For heterologous expression in yeast, *ACA12* and *ACA12-GFP* coding sequences were amplified by PCR (Robocycler gradient 40, Stratagene) using ps 391 as template and cloned into the *pYES2* vector (Online Resource 1). Generation of N211D and R334E mutants of *ACA12-GFP* was performed by site-directed mutagenesis using the Quickchange site-directed mutagenesis kit (Stratagene) according to the manufacturer's protocol, using WT *ACA12-GFP* full length cDNA inserted in the *pYES2* as a template (Online Resource 1).

Plant transformation

Plants were transformed with *Agrobacterium tumefaciens* strain GV3101 using the floral-dip method (Clough and Bent 1998). For the *pGreenII* vector, the *Agrobacterium* also included a *pSOUP* helper plasmid with a tetracycline resistance gene (Hellens et al. 2000). T1 seedlings were grown on 0.5× MS medium (pH 5.7) containing 1 % agar, 0.05 % MES, and 25 μg/ml hygromycin (*pGreenII* based constructs) or 50 μg/ml kanamycin (*pBIN* based vector) to identify stable transgenic lines.

Confocal microscopy

Root images of 7–10 day old dark-grown seedlings expressing ACA12-GFP under the control of the 35S promoter were collected using an Olympus IX81 FV1000 confocal microscope run by the Olympus FluoView 1.07.03.00 software package equipped with a 60× objective (numerical aperture 1.42) (Fig. 1A–C) or a confocal microscope Leica TCS SP2 AOBS with a 40× oil-immersion objective (Fig. 1D–I). For co-localization experiments seedlings were exposed for 5–10 min to 4 μM FM4-64 dye freshly prepared solution (Bolte et al. 2004). Excitation at wavelengths of 488 nm was provided with an Argon-Ion laser. A spectral emission range of 500–600 nm was used for GFP imaging, while a 500–530 nm (GFP) and a 625–665 nm (FM4-64) range were used in co-localization experiments.

Yeast strains, transformation, and growth media

cDNAs coding for *ACA12*, *ACA12-GFP*, and *ACA12-GFP* mutants were in *pYES2* vector (Invitrogen) under the control of the GAL1 promoter. Plasmids were used to transform *Saccharomyces cerevisiae* strain K616 [*MATa pmr1*::*HIS3 pmc1*::*TRP1 cnb1*::*LEU2, ade2, ura3* (Cunningham and Fink 1994)] using a lithium acetate/single-stranded DNA/polyethylene glycol protocol and transformants were selected for uracil prototrophy by plating on complete synthetic medium lacking uracil (SC-URA) as described (Bonza et al. 2004). To induce protein expression, the different yeast strains were grown in SC-URA medium containing 2 % (w/v) galactose, 1 % (w/v) raffinose, 50 mM succinic acid/Tris (pH 5.5), 0.7 % (w/v) yeast nitrogen base and 10 mM $CaCl_2$, for 24 h at 20 °C.

Complementation of the yeast mutant K616

For complementation experiments, single colonies of the different strains were grown in a SC-URA medium containing 2 % (w/v) glucose, 50 mM succinic acid/Tris (pH 5.5), 0.7 % (w/v) yeast nitrogen base and 10 mM $CaCl_2$; cultured cells were pelletted, washed and diluted with water to $A_{600} = 1 - 0.3 - 0.1$. Five μL of each dilution were spotted on solid SC-URA medium containing 2 % (w/v) galactose, 1 % (w/v) raffinose, 50 mM succinic acid/Tris (pH 5.5), 0.7 % (w/v) yeast nitrogen base supplemented with 10 mM $CaCl_2$ or 5 mM EGTA. As controls, yeast strain K616 transformed with the *pYES2* empty vector or expressing full length ACA8 or the Δ74-ACA8 truncated mutant were used (Bonza and Luoni 2010). Growth was recorded after 3–8 days of incubation at 20 °C.

Isolation of yeast microsomes

Microsomal fraction was isolated as previously reported (Fusca et al. 2009) except that yeast cells were lysed using a Cell Disruptor (Constant Systems Ltd) operating

at 27 psi. Protein concentration was determined using the Bio-Rad assay (Bio-Rad) with γ-globulin as standard.

ACA12 and ACA12-GFP purification by CaM-affinity chromatography

CaM-affinity purification was performed as described (Fusca et al. 2009) with slight modifications. Proteins (100 mg) from yeast microsomes expressing ACA12 or ACA12-GFP were incubated with *n*-dodecyl β-D-maltoside (4 mg detergent ml^{-1}: 4 mg protein ml^{-1}) at 25 °C for 30 min in a solubilization medium containing 5 % (v/v) glycerol, 50 mM Tris–HCl, pH 7.5, 1 mM *p*-aminobenzamidine, 2 mM DTT, 1.5 mM ATP, 2 mM $CaCl_2$, 1 mM $MgSO_4$, 125 mM NaCl, supplemented with 5 μg ml^{-1} leupeptin, 5 μg ml^{-1} pepstatin, 5 μg ml^{-1} chymostatin immediately before use. The sample was then centrifuged 1 h at 110,000*g* at 4 °C; the supernatant recovered and incubated overnight under gentle rotation at 4 °C with 0.8 ml of CaM-Sepharose (GeHealthcare) previously equilibrated with solubilization medium supplemented with 37.5 μg ml^{-1} Brij 58. After removal of the unbound fraction, the resin was washed with 10 ml of washing medium containing 10 % (v/v) glycerol, 20 mM Mops-KOH, pH 7.5, 1 mM *p*-aminobenzamidine, 2 mM DTT, 0.25 mM NaBr, 37.5 μg ml^{-1} Brij 58, 5 μg ml^{-1} leupeptin, 5 μg ml^{-1} pepstatin, 5 μg ml^{-1} chymostatin, 100 μM $CaCl_2$, 100 μM $MgSO_4$; second and third washes were performed in the same medium but in the absence of $CaCl_2$ and $MgSO_4$ (Bonza et al. 1998; Fusca et al. 2009). CaM-bound proteins were eluted in 2.5 ml of 5 mM Mops-KOH, pH 7.5, 37.5 μg ml^{-1} Brij 58, 10 % (v/v) glycerol and 2 mM EGTA, followed by 1.5 ml of the same solution. The EGTA-eluted fractions were supplemented with 2 mM $CaCl_2$, pooled and concentrated 10- to 20-fold on Vivaspin ultrafiltration spin columns, 30 kDa cut-off (Sartorius), to a final concentration of 250–600 μg ml^{-1}. The EGTA-eluted fraction was immediately used for assay of Ca^{2+}-ATPase activity or re-lipidated by overnight incubation at 4 °C under gentle rotation with soybean phosphatidylcoline (PC). PC, dissolved in 20 mg ml^{-1} Brij 58 and then diluted ten times in water to a final concentration of 8.5 mM, was supplied at 500 μM (Gourdon et al. 2011). Re-lipidated ACA12 maintains the same Ca^{2+}-ATPase activity of the freshly purified protein (data not shown).

Electrophoresis and western blot analysis

SDS–PAGE and western blotting were performed as previously described (Bonza et al. 2000). ACA12-GFP decoration was performed incubating the nitrocellulose membrane for 1 h at 25 °C with the HisProbe-HRP, a nickel activated derivative of horseradish peroxidase (Thermo Scientific) which can bind to the His tag fused to the C-terminus of the protein. The probe was diluted 1:5,000 in 0.05 % (w/v) polyoxy-ethylene(20)sorbitan monolaurate, 0.15 M NaCl, 20 mM Tris–HCl, pH 7.4. ECL signal was acquired and quantified by the Fluor-Chem™SP Imaging System and AlphaEaseFC software (Alpha Innotech). Alternatively, gel was stained with silver impregnation (ProteoSilver™ Silver Stain Kit, Sigma Aldrich) or Coomassie blue staining method.

Assays of ACA12 activity

Activity of purified ACA12 (400–600 ng for each sample) was measured as Ca^{2+}-dependent Mg-ATP hydrolysis as previously described (Bonza and Luoni 2010). Ca^{2+}-dependent ATPase activity was evaluated as the difference between activity measured in the presence of 40 μM free Ca^{2+} and that measured in the absence of Ca^{2+} in the assay medium. Samples were incubated at 25 °C for 60 min, during which the reaction proceeds linearly. All the assays were performed at least three times, with three replicates.

Results

ACA12 is a functional PM Ca^{2+}-ATPase

To define the intracellular localization of ACA12, transgenic plants expressing GFP-fused ACA12 (ACA12-GFP) under the control of the 35S promoter were generated and analyzed by confocal microscopy. Figure 1 shows that GFP fluorescence localizes at the periphery of the cells, consistent with a PM localization of ACA12 (panels A, B, D, G). To confirm this indication, roots were briefly (5–10 min) exposed to the FM4-64 dye, which under these conditions selectively labels the PM (Bolte et al. 2004): GFP and FM4-64 signals clearly co-localize at cell periphery (panels D–I).

Based on these results we tested whether ACA12 was able to complement the pollen fertility phenotype of an *aca9* null mutant. ACA9 is a PM localized isoform primarily expressed in pollen and its deletion has been shown to reduce growth of pollen tubes with high frequency of aborted fertilization leading to a threefold reduction in seed set (Schiøtt et al. 2004). Results in Fig. 2 show that the expression of *ACA12* rescues the *aca9* mutant, while that of *ACA2*, which encodes for an ACA isoform localized at the endoplasmic reticulum (Hong et al. 1999), is unable to complement the defect. Consistent with this difference in rescue potential, ACA12-YFP was observed to localize at the PM in pollen, whereas ACA2 was limited to the endomembranes (Online Resource 2). Together, these results indicate that ACA12 is a functional PM Ca^{2+} pump.

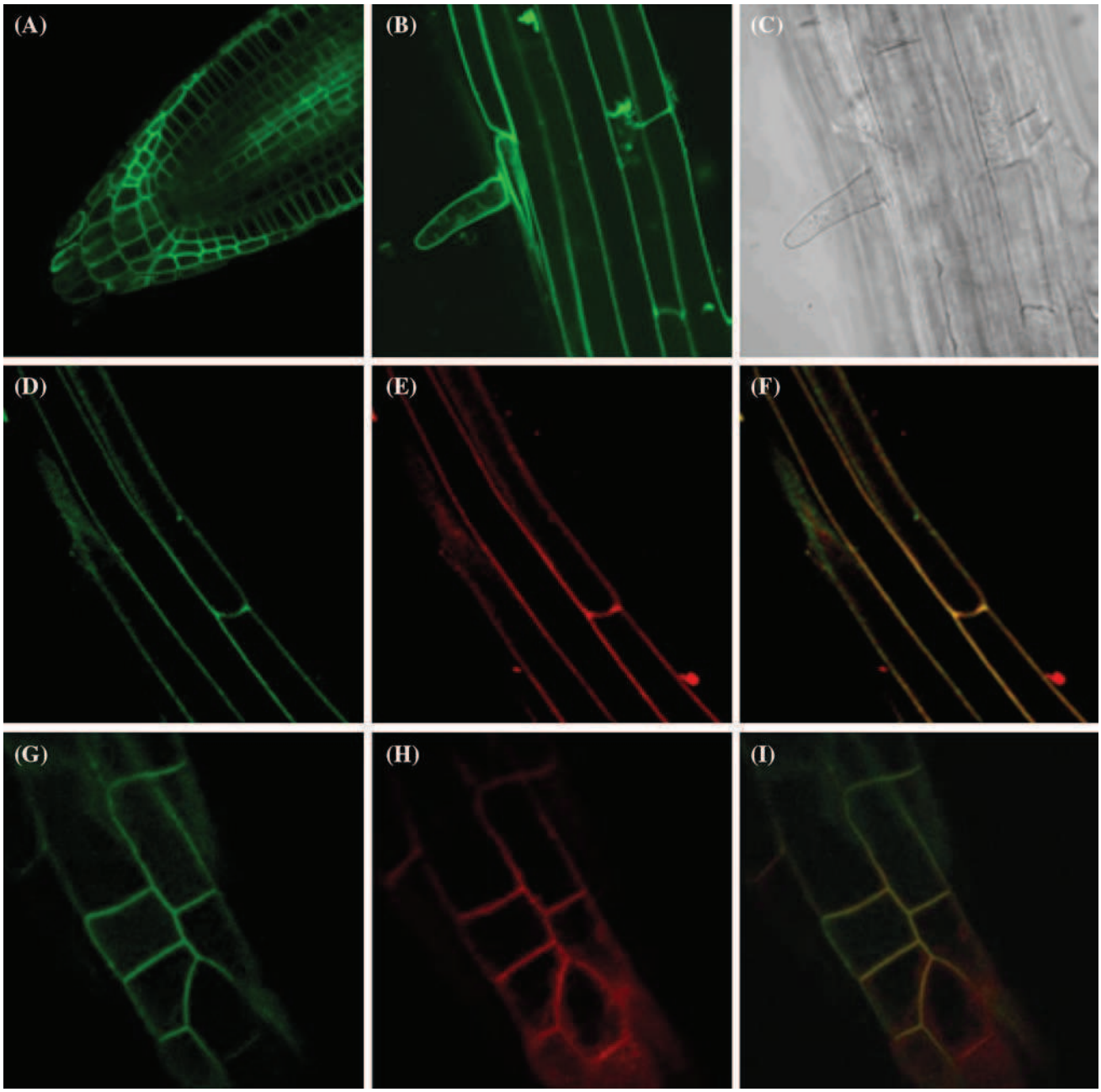

Fig. 1 ACA12-GFP is PM localized. **A**, **B**, **D** and **G**: GFP fluorescence; **C**: phase contrast image; **E** and **H**: fluorescence of FM4-64 dye; **F** and **I** merging. **A**: root tip; **B**, **C**, **D**, **E** and **F**: maturation root zone; **G**, **H** and **I**: elongation root zone

Expression of ACA12 in yeast and protein purification

To biochemically characterize ACA12, plasmids encoding *ACA12* and *ACA12-GFP* (the latter contains also a 6His tag) under the control of the GAL1 promoter were used to transform *Saccharomyces cerevisiae* strain K616, which lacks endogenous Ca^{2+}-ATPases (Cunningham and Fink 1994). After induction of the yeast strain carrying *ACA12-GFP*, microsomes were isolated and solubilized microsomal proteins were subjected to SDS-PAGE, blotted and decorated with the HisProbe-HPR (Fig. 3). After standard induction conditions (24 h at 30 °C) the probe recognizes only a very faint band of the expected molecular mass (141 kDa). However, an increase in accumulation was observed if the temperature during induction was lowered to 20 °C. Nevertheless, even in this condition, ACA12-GFP expression levels were very low compared to that of another ACA isoform: the signal in the lane containing a His-tagged Δ109-ACA8 is much stronger than that of ACA12-GFP, although 100-fold more microsomal proteins were loaded in the latter

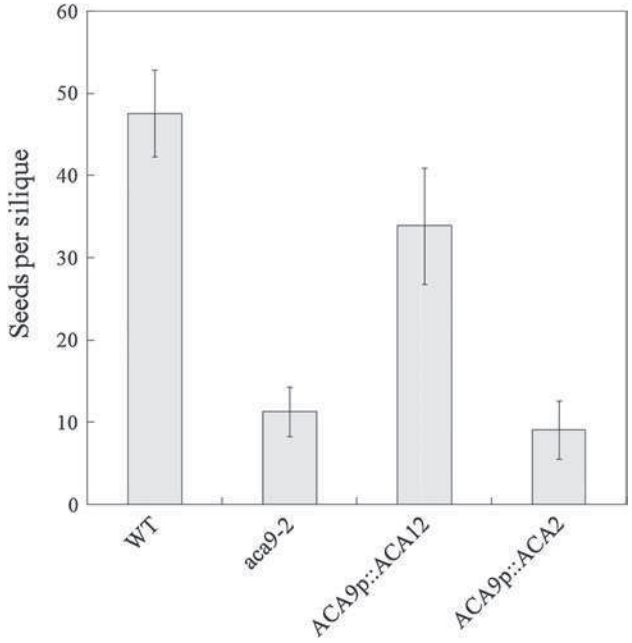

Fig. 2 ACA12 rescues the reduced fertility phenotype of *aca9* null mutants. Average seed set per silique was determined for plants grown under green house conditions. All wild type (WT), *aca9-2*, and transgenic lines were created using an *A. thaliana* ecotype WS background. Seeds were counted from 10 consecutive siliques on the primary bolt. Multiple plants were used for WT (N = 3), and *aca9-2* (N = 4), and one each for 20 independent transgenic plant lines harboring an ER control *ACA2* construct (ps 585), and 26 independent transgenic plant lines harboring an *ACA12* construct (ps 688). Using another knockout line (*aca9-1*) transformed with the same *ACA12* construct, an equivalent level of restored seed set was visually confirmed in a separate experiment. Four representative transgenic lines for ACA12-TAP2(YFP) in *aca9-2* are ss 2099-2102, and ss 2103–2106 for the control ACA2-GFP in *aca9-2*

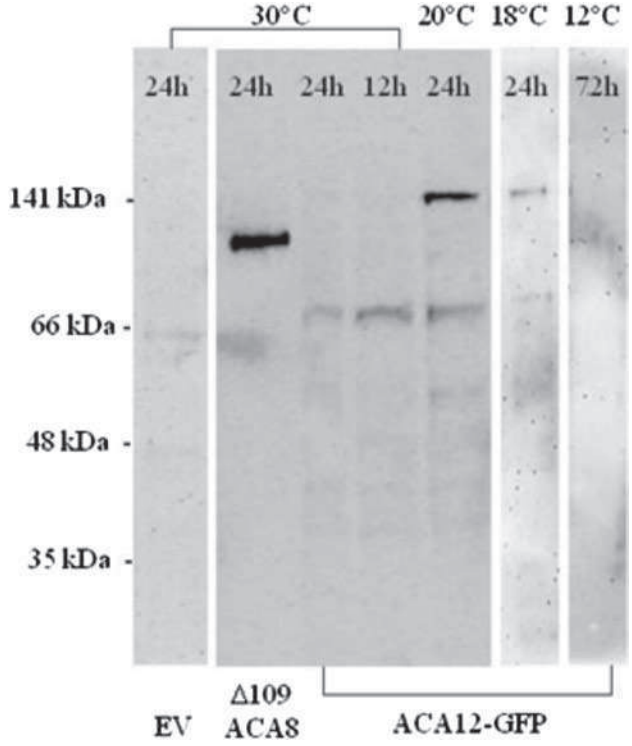

Fig. 3 Expression of ACA12-GFP in yeast strain K616. K616 yeast transformed with an empty *pYES2* vector (EV), with *Δ109-ACA8-6His* or with *ACA12-GFP* was galactose-induced at the specified temperatures for the indicated times; solubilized microsomal proteins (30 μg for EV and ACA12-GFP and 0.3 μg for Δ109-ACA8) were subjected to SDS-PAGE, blotted and decorated with the HisProbe-HPR

case; moreover also under this conditions the HisProbe-HPR labels several smaller bands (the most prominent of about 70 kDa) indicative of ACA12-GFP degradation. Attempts to improve ACA12-GFP expression by further lowering the temperature of induction till 12 °C (Fig. 3), by lowering Ca^{2+} concentration in the medium during induction to possibly select cells efficiently expressing the heterologous Ca^{2+}-ATPase (Cunningham and Fink 1994), or by changing promoter were unsuccessful (data not shown).

K616 yeast strain, being devoid of endogenous Ca^{2+}-ATPases, is unable to grow in Ca^{2+}-depleted media unless it expresses a deregulated form of ACA (Curran et al. 2000; Bonza et al. 2004; Baekgaard et al. 2006). We checked whether at 20 °C ACA12-GFP allows K616 growth in a Ca^{2+}-depleted medium: Fig. 4 shows that K616 yeast expressing ACA12-GFP grows in the presence of 5 mM EGTA nearly as well as that expressing the deregulated Δ74-ACA8 mutant, while that expressing WT ACA8 is unable to grow under these conditions (Bonza et al. 2004). This result indicates that the yeast expressed ACA12-GFP protein is functional and not auto-inhibited. A rescue was also obtained by K616 transformation with an untagged *ACA12*, indicating that the WT protein is also expressed in a functional form and that the addition of the GFP did not somehow cause the tagged pump to become de-regulated.

Given the low expression level of ACA12-GFP (and probably also of ACA12, see below) it is extremely unlikely that yeast growth under selective conditions is enabled by some ACA12 fragment which has lost the auto-inhibitory domain. However, to evaluate this possibility, we purified ACA12 from yeast using CaM-affinity chromatography (Bonza et al. 1998, 2000; Fusca et al. 2009; Bonza and Luoni 2010), and tested its biochemical properties.

Panel A in Fig. 5 shows the main fractions obtained from purification of ACA12-GFP, which can be easily monitored thanks to the His tag. Upon overnight incubation with CaM-Sepharose of the microsomal proteins solubilized from K616 cells expressing ACA12-GFP, a relevant portion of the protein remains associated to the resin (compare lane 1 with lane 2, on which comparable amounts of the solubilized microsomal fraction and of the unbound fraction were loaded). The intact ACA12-GFP protein (141 kDa) is eluted upon Ca^{2+}-chelation with 2 mM EGTA (lane 3),

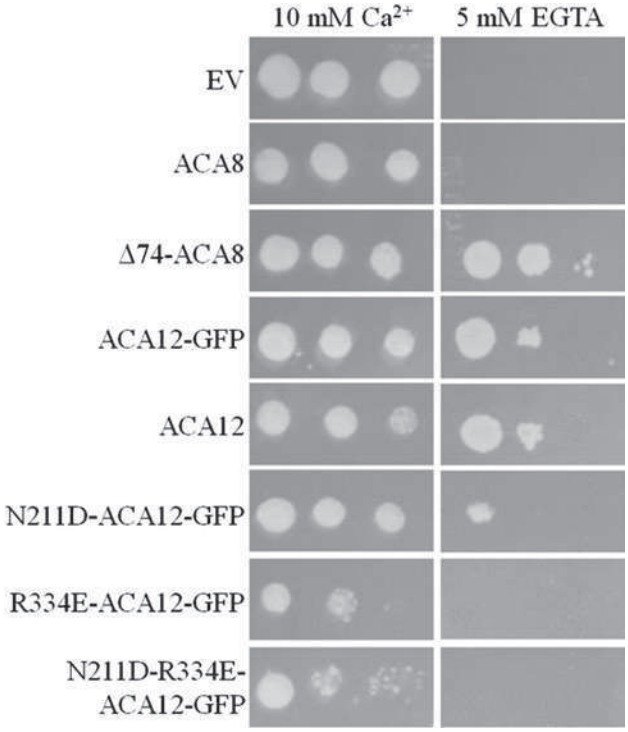

Fig. 4 ACA12 complements the phenotype of Ca^{2+}-ATPase deficient yeast K616 strain. Precultures of K616 transformed with the specified constructs grown in synthetic complete medium lacking uracil (SC-URA), 2 % (w/v) glucose, 10 mM $CaCl_2$ were pelletted, washed and diluted with water. Five µl of cells at $A_{600} = 1.0$—or serial 1:3 dilutions—were spotted on SC-URA, 2 % (w/v) galactose, 1 % (w/v) raffinose, supplemented with 10 mM $CaCl_2$ or 5 mM EGTA. All media were supplemented with 50 mM succinic acid/Tris (pH 5.5), 0.7 % (w/v) yeast nitrogen base. Plates were incubated for 8 days at 20 °C. Results are from one experiment representative of three

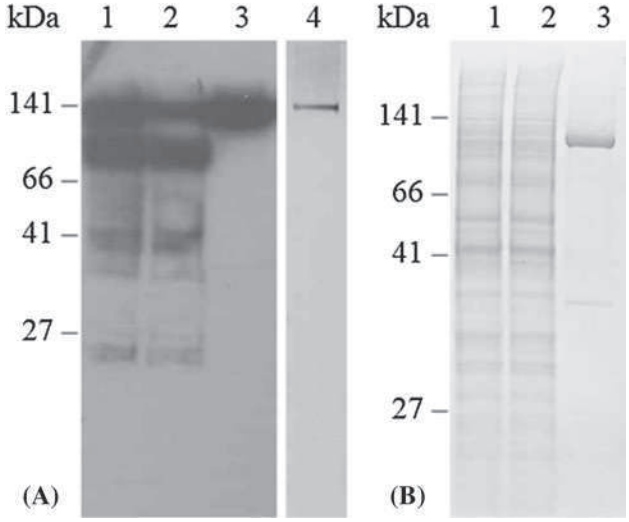

Fig. 5 Purification of ACA12-GFP (*panel A*) and ACA12 (*panel B*) by CaM-Sepharose affinity. Yeast microsomal proteins (100 mg), solubilized with *n*-dodecyl β-D-maltoside, were incubated overnight with CaM-Sepharose; after collection of the unbound protein fraction, the resin was washed as described in the Materials and Methods and CaM-bound proteins were eluted with 4 ml of elution buffer containing 2 mM EGTA. *Panel A*: *lane 1*, 10 µl of solubilized microsomal proteins (40 µg); *lane 2*, 10 µl of the unbound protein fraction; *lane 3*, 9 µl of the EGTA-eluted fraction; *lane 4*, 1 µl of the EGTA-eluted fraction concentrated ten-fold. Fractions were subjected to SDS-PAGE, blotted and decorated with the HisProbe-HPR (*lanes 1–3*) or subjected to SDS-PAGE and silver-stained (*lane 4*). *Panel B*: *lane 1*, 10 µl of solubilized microsomal proteins (40 µg); *lane 2*, 10 µl of the unbound protein fraction; *lane 3*, 3.5 µl of the EGTA-eluted fraction concentrated 20-fold. Fractions were subjected to SDS-PAGE and stained with *Comassie blue*

Table 1 *Activity of CaM-affinity purified ACA12*

Assay conditions	Ca^{2+}-ATPase activity (nmol Pi min^{-1} mg^{-1} protein)
ATP	289 ± 27
ATP + 1 µM CaM	303 ± 31
ATP + 10 µM CaM	309 ± 29
ATP + 200 µM vanadate	3 ± 1
ITP	25 ± 3

Ca^{2+} -ATPase activity of ACA12 was measured as described in the Materials and Methods. Results (plus or minus standard error of the mean) are from three experiments, each with three replicates, performed on different purified fractions

while the His-tagged lower molecular weight bands are undetectable in the EGTA-eluted fraction. Moreover, the 141 kDa band is by far the most prominent after SDS-PAGE and silver staining of the EGTA-eluted fraction (lane 5), indicating that this procedure allows the recovery of quite pure ACA12-GFP protein, albeit in tiny amounts (ca. 1 µg protein per mg of microsomal protein). Upon application of the same purification procedure to microsomes from K616 cells expressing WT ACA12 (panel B in Fig. 5), a band of 113 kDa is prominent in the EGTA-eluted fraction (lane 3), indicating that CaM-affinity also allows purification of the untagged ACA12 protein, albeit still with low yield (ca. 1 µg ACA12 per mg of microsomal protein).

The purified ACA12 protein has Ca^{2+}-ATPase activity insensitive to CaM even when supplied at 10 µM concentration (Table 1). ACA12 activity is inhibited by vanadate, a well known inhibitor of P-type ATPases, but in contrast with other ACAs (Bonza and De Michelis 2011 and references therein) is virtually unable to use ITP as an alternative substrate (Table 1). As with other ACAs, ACA12 is inhibited by micromolar concentrations of eosin Y (Fig. 6), a fluorescein derivative which acts as a competitive inhibitor with respect to the nucleoside triphosphate substrate (De Michelis et al. 1993); however, the effective concentrations are about 2 order of magnitude higher that those required to inhibit ACA8 (Bonza et al. 2004).

The specific activity of the purified ACA12 is low as compared to the CaM-stimulated activity of ACA8 purified

under the same conditions which ranges between 2 and 3 μmol $min^{-1}mg^{-1}$ protein (Bonza and Luoni 2010, unpublished data from the authors laboratory). This low activity is very unlikely to be an intrinsic characteristic of ACA12, since it is able to complement the K616 phenotype despite its very low expression level. Rather, it is probably due to protein damage during purification: indeed, the activity of purified ACA12 decreases by 50–80 % upon freezing and storage at −80 °C (data not shown) and can be preserved overnight only by maintaining the protein at 4 °C in the presence of phosphatidylcholine (100-fold molar excess). We tried to improve ACA12 activity by adding phospholipids during the solubilization and/or purification procedure, without success. The finding that the expression level of ACA12-GFP in mature leaves of transgenic plants expressing ACA12-GFP under the control of the 35S promoter is fairly low (data not shown) suggests that protein instability might be an intrinsic feature of ACA12.

Single point mutations of ACA12 suppress its ability to complement the phenotype of the K616 yeast strain

Alignment of ACA12 (Fig. 7) with the other ACAs of Arabidopsis shows that two residues crucial for auto-inhibition of type 2B Ca^{2+}-ATPases and conserved in all members of the other three clusters, are variant in ACA12 and ACA13: ACA12 N211 aligns with an Asp, and R334 with a Glu in ACAs belonging to the other three clusters. In studies on other ACA isoforms as well as on a PMCA, single point mutations of each of these two acidic residues, respectively localized at the edge of TM2 and of TM3, generates constitutively active proteins, insensitive to CaM (Curran et al. 2000; Bredeston and Adamo 2004; Fusca et al. 2009). We generated ACA12 mutants in which N211 was mutated to Asp and/or R334 to Glu: all mutants are expressed in K616 yeast at levels similar to that of the WT protein (Online Resource 3). While the N211D-ACA12 only partially impairs the ability of the construct to rescue the growth phenotype (Fig. 4), there was no rescue with a single substitution of R334E-ACA12 or a double N211D-R334E substitution.

Discussion

In this paper we perform a characterization of ACA12 and we show that it has biochemical and regulatory features distinct from other characterized ACAs, potentially providing a unique biological function for plant cells. First, we demonstrate that it is localized at the PM: this is shown by confocal microscopy of plants expressing the ACA12-GFP or -YFP fusion proteins (Fig. 1 and Online Resource 2), which co-localizes with the PM dye FM4-64 (Bolte et al. 2004), in agreement with the observations of Frei dit

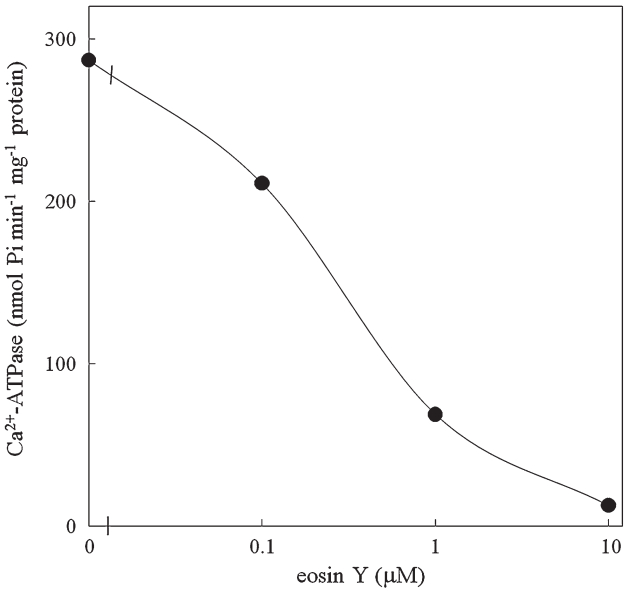

Fig. 6 Effect of eosin Y on ACA12 activity. Ca^{2+}-dependent ATPase activity of ACA12 was measured as described in the Materials and Methods, in the presence of the specified eosin Y concentrations. Results are from one experiment, representative of three

Frey et al. (2012), and by the ability of ACA12—expressed under the *ACA9* promoter—to rescue the phenotype of a null mutant of *ACA9* (Fig. 2), a PM isoform primarily expressed in pollen (Schiøtt et al. 2004). The latter result also provides the first demonstration that ACA12 is a functional Ca^{2+}-ATPase.

ACA12 and 13 are 40–50 % similar to the other eight ACA isoforms in Arabidopsis, which together can be divided into 4 different clusters. However, their sequence is highly divergent in the regulatory N-terminus which contains the auto-inhibitory domain and the CaM-binding sites: in this region similarity between ACA12 and ACA13 is only 18 % and their similarity to other ACAs ranges between 9 and 16 %. In particular only one of the two anchor residues in the high affinity CaM-binding site (W28 of ACA12) is conserved. Nevertheless, ACA12 binds CaM and this has allowed its purification by CaM-affinity chromatography (Fig. 5).

ACA12 differs from the other ACAs characterized so far for being virtually unable to use ITP as a substrate alternative to ATP, and for being less sensitive to inhibition by the fluorescein derivative eosin Y (Table 1, Fig. 6). Since fluorescein and its derivatives are competitive inhibitors of P-type ATPases, which act by binding to a conserved Lys residue in the nucleotide-binding domain, these results suggest that the conformation of this domain on ACA12 is more similar to that of other P-type ATPase—which are ATP-specific and less sensitive to inhibition by fluorescein derivatives—than to that of ACA isoforms pertaining to the

```
ACA1   201 HDGLGIVASILLVVFVTATSDYRQSLQFKDLDAEKKKI 238
ACA2   199 HDGLGIAASILLVVFVTATSDYRQSLQFRDLDKEKKKI 236
ACA7   200 HDGLGIVASILLVVFVTATSDYRQSLQFRDLDKEKKKI 277
ACA4   196 YDGTGILLSILLVVMVTAISDYKQSLQFRDLDREKKKI 233
ACA11  196 YDGTGILLSIILVVMVTAISDYKQSLQFRDLDREKKKI 233
ACA8   219 YDGGSIAFAVILVIVVTAVSDYKQSLQFQNLNDEKRNI 256
ACA9   220 LDGGSIAFAVLLVIVVTAVSDYRQSLQFQNLNDEKRNI 257
ACA10  219 YDGISIAFAVLLVIVVTATSDYRQSLQFQNLNEEKRNI 256
ACA12  191 YEGGSIFVAVFLVIVVSALSNFRQERQFDKLSKISNNI 228
ACA13  186 YDGGSIFVAVFLVVAVSAVSNFRQNRQFDKLSKVSSNI 223

ACA1   332 LMATLSEGGDDETPLQVKLNGVATIIGKIGLFFAVITF 369
ACA2   330 LMATLTEGGDDETPLQVKLNGVATIIGKIGLFFAVVTF 367
ACA7   331 LMATLSEGGDDETPLQVKLNGVATIIGKIGLSFAIVTF 368
ACA4   327 LMETLVDGGEDETPLQVKLNGVATIIGKIGLSFAVLTF 364
ACA11  327 LMDTLSEGGEDETPLQVKLNGVATIIGKIGLGFAVLTF 364
ACA8   351 LMASISEDNGEETPLQVRLNGVATFIGSIGLAVAAAVL 388
ACA9   351 LMASISEDTGEETPLQVRLNGLATFIGIVGLSVALVVL 388
ACA10  351 LMASVSEDNGGETPLQVRLNGVATFIGIVGLTVAGVVL 388
ACA12  323 TMSSINQDSSERTPLQVRLDTLTSTIGKIGLTVAALVL 360
ACA13  318 MMSHISRDTNEQTPLQSRLDKLTSSIGKVGLLVAFLVL 355
```

Fig. 7 Alignment of Arabidopsis ACA isoforms. *Top panel* TM2 (underlined in ACA12) and beginning of the small cytoplasmic loop, with the variant N211 of ACA12 highlighted (*white on black background*); *bottom panel* end of the small cytoplasmic loop and TM3 (underlined in ACA12) with the variant R344 of ACA12 highlighted (*white on black background*). Sequence alignment was performed using ClustalW

other three clusters (De Michelis et al. 1993; Bonza et al. 2004; Bonza and De Michelis 2011).

The activity of the purified ACA12 protein could not be activated by CaM (Table 1). Moreover, despite its low expression level, ACA12 was able to complement the K616 phenotype, making it able to grow in the presence of 5 mM EGTA (Fig. 4), as only deregulated mutants of other ACA isoforms are able to do (Harper et al. 1998; Chung et al. 2000; Geisler et al. 2000b; Hwang et al. 2000; Sze et al. 2000; Bonza et al. 2004; Kabala and Klobus 2005; Schiøtt and Palmgren 2005; Baekgaard et al. 2006; Lee et al. 2007). Taken together, these results clearly indicate that ACA12 is a deregulated isoform of Arabidopsis type 2B Ca^{2+}-ATPase. This property may be connected to the lack of two acidic residues, conserved in other subgroups of ACAs as well as in animal type 2B Ca^{2+}-ATPases, at the edge of TM2 and of TM3 respectively. Residue N211 of ACA12 aligns with a conserved Asp and residue R334 with an equally conserved Glu (Fig. 7): in different ACA isoforms, as well as in an animal pump isoform, mutation of these acidic residues generates a deregulated pump almost insensitive to further activation by CaM (Curran et al. 2000; Bredeston and Adamo 2004; Fusca et al. 2009). The N211D-ACA12 mutant allows some growth of the K616 yeast strain in low Ca^{2+} medium, while R334E-ACA12 as well as the double mutant N211D-R334E-ACA12 are unable to complement the K616 phenotype (Fig. 4); since the mutant proteins are expressed to levels similar to that of WT ACA12, the simplest interpretation of these results is that introduction of a negatively charged residue at one, or better both, of these positions restore in ACA12 the auto-inhibited conformation typical of other type 2B Ca^{2+}-ATPases in the absence of CaM. However, since the activity of the R334E mutant purified with the same protocol used for the WT protein was barely detectable also in the presence of CaM (data not shown), the possibility exists—albeit unlikely since most ACA isoforms have a Glu at this position—that the mutation generates a non functional protein.

The question of the role that a deregulated ACA isoform as ACA12 can play in the physiology of the plant remains open. A careful analysis of gene knockouts for ACA12 has not yet been reported. While our study did not detect any obvious phenotype resulting from the expression of ACA12 under a 35S or ACA9 promoter, we did not conduct a systematic analysis of different growth conditions. However, expression profiling through microarrays shows that, in contrast to the relatively constant and redundant expression of most ACA isoforms, under normal growth conditions ACA12 transcripts are barely detectable throughout plant development. Nevertheless, ACA12 might be expressed under normal conditions in some specific cell type, such as guard cells [http://bar.utoronto.ca/efp_arabidopsis/cgi-bin/efpWeb.cgi (Winter et al. 2007)].

One potential hint on a possible role of ACA12 in plant development comes from the observation that, when transiently co-expressed in *N. benthamiana* leaves, ACA12 interacts at the PM with the brassinosteroid receptor BRI1 and with CLV1, which plays a central role in the control of the size of the central stem cell pool in the shoot apical

meristem (Gish and Clark 2011; Frei dit Frey et al. 2012). However the same ability is shared by ACA8 (Frei dit Frey et al. 2012), a widely expressed PM isoform (Cerana et al. 2006). Since both BRI1 and CLV1 are members of the large family of receptor-like kinases (RLK) (Gish and Clark 2011), the two pumps might be substrate of their kinase activity. In the case of ACA8 it is known that this pump is phosphorylated in vivo at several Ser residues in the regulatory N-terminus and that phosphorylation can affect both auto-inhibition and CaM-binding (Giacometti et al. 2012 and references therein). Although most of these Ser residues are not conserved in ACA12, we cannot exclude that phospho-dephosphorylation might also impact ACA12 activity, and that the yeast expressed enzyme might have properties different from that expressed in planta.

RLKs constitute a large gene family in plants, with more than 600 members in Arabidopsis, and are involved in diverse ligand-mediated signaling pathways (Shiu and Bleecker 2001). In particular, several RLKs have been shown to be receptor proteins involved in perception of pathogen-associated molecular patterns (Boller and Felix 2009; Ranf et al. 2011); one of the first events in defense signaling is a transient increase of cytosolic free Ca^{2+} concentration (Ranf et al. 2011). Interestingly, interactomics screening by the split ubiquitin test has identified four orphan RLKs as ACA12 interactors (http://cas-biodb.cas.unt.edu/project/mind/search.php). Moreover, ACA12 expression is dramatically induced upon exposure to pathogens [(Boursiac and Harper 2007); http://bar.utoronto.ca/efp_arabidopsis/cgi-bin/efpWeb.cgi (Winter et al. 2007)], suggesting that it may be involved in the adaptive response to these stress signals: expression of a deregulated PM Ca^{2+}-ATPase may impact on the shape of pathogen-induced Ca^{2+} transient (Boller and Felix 2009; Ranf et al. 2011) and consequently on the response of the plant to a new pathogen attack.

Acknowledgments This work was supported by grants to JFH from NSF DBI-0420033 for stress-dependent phenotype screens, NIH 1RO1 GM070813-01 for studies on pollen tube tip growth, and DOE DE-FG03-94ER20152 for studies on membrane biogenesis and genetic analyses of ACAs. Confocal microscopy was made possible by support at UNR from NIH COBRE grant RR024210. We thank Prof. Anna Moroni, Dipartimento di Bioscienze, Università degli Studi di Milano (Italy), for her generous support during completion of this work, Woo Sik Chung for assistance in cloning *ACA12* from plant genomic DNA and Kathy Troung for assistance in plant rescue experiments.

References

Axelsen KB, Palmgren MG (1998) Evolution of substrate specificities in the P-type ATPase superfamily. J Mol Evol 46(1):84–101

Baekgaard L, Luoni L, De Michelis MI, Palmgren MG (2006) The plant plasma membrane Ca^{2+} pump ACA8 contains overlapping as well as physically separated autoinhibitory and calmodulin-binding domains. J Biol Chem 281(2):1058–1065. doi:10.1074/jbc.M508299200

Baxter I, Tchieu J, Sussman MR, Boutry M, Palmgren MG, Gribskov M, Harper JF, Axelsen KB (2003) Genomic comparison of P-type ATPase ion pumps in *Arabidopsis* and rice. Plant Physiol 132(2):618–628. doi:10.1104/pp.103.021923

Bevan M (1984) Binary Agrobacterium vectors for plant transformation. Nucleic Acids Res 12(22):8711–8721

Boller T, Felix G (2009) A renaissance of elicitors: perception of microbe-associated molecular patterns and danger signals by pattern-recognition receptors. Annu Rev Plant Biol 60:379–406. doi:10.1146/annurev.arplant.57.032905.105346

Bolte S, Talbot C, Boutte Y, Catrice O, Read ND, Satiat-Jeunemaitre B (2004) FM-dyes as experimental probes for dissecting vesicle trafficking in living plant cells. J Microsc 214(Pt 2):159–173. doi:10.1111/j.0022-2720.2004.01348.x

Bonza MC, De Michelis MI (2011) The plant Ca^{2+}-ATPases repertoire: biochemical features and physiological functions. Plant Biol 13:421–430

Bonza MC, Luoni L (2010) Plant and animal type 2B Ca^{2+}-ATPases: evidence for a common auto-inhibitory mechanism. FEBS Lett 584(23):4783–4788. doi:10.1016/j.febslet.2010.11.008

Bonza C, Carnelli A, Ida De Michelis M, Rasi-Caldogno F (1998) Purification of the plasma membrane Ca2+-ATPase from radish seedlings by calmodulin-agarose affinity chromatography. Plant Physiol 116(2):845–851

Bonza MC, Morandini P, Luoni L, Geisler M, Palmgren MG, De Michelis MI (2000) At-ACA8 encodes a plasma membrane-localized calcium-ATPase of *Arabidopsis* with a calmodulin-binding domain at the N terminus. Plant Physiol 123(4):1495–1506

Bonza MC, Luoni L, De Michelis MI (2004) Functional expression in yeast of an N-deleted form of At-ACA8, a plasma membrane Ca^{2+}-ATPase of Arabidopsis thaliana, and characterization of a hyperactive mutant. Planta 218(5):814–823. doi:10.1007/s00425-003-1160-y

Bose J, Pottosin II, Shabala SS, Palmgren MG, Shabala S (2011) Calcium efflux systems in stress signaling and adaptation in plants. Front Plant Sci 2:85. doi:10.3389/fpls.2011.00085

Boursiac Y, Harper JF (2007) The origin and function of calmodulin regulated Ca^{2+} pumps in plants. J Bioenerg Biomembr 39(5–6):409–414. doi:10.1007/s10863-007-9104-z

Boursiac Y, Lee SM, Romanowsky S, Blank R, Sladek C, Chung WS, Harper JF (2010) Disruption of the vacuolar calcium-ATPases in *Arabidopsis* results in the activation of a salicylic acid-dependent programmed cell death pathway. Plant Physiol 154(3):1158–1171. doi:10.1104/pp.110.159038

Bredeston LM, Adamo HP (2004) Loss of autoinhibition of the plasma membrane Ca^{2+} pump by substitution of aspartic 170 by asparagin. Activation of plasma membrane calcium ATPase 4 without disruption of the interaction between the catalytic core and the C-terminal regulatory domain. J Biol Chem 279(40):41619–41625. doi:10.1074/jbc.M403116200

Cerana M, Bonza MC, Harris R, Sanders D, De Michelis MI (2006) Abscisic acid stimulates the expression of two isoforms of plasma membrane Ca^{2+}-ATPase in *Arabidopsis thaliana* seedlings. Plant Biol (Stuttg) 8(5):572–578. doi:10.1055/s-2006-924111

Chung WS, Lee SH, Kim JC, Heo WD, Kim MC, Park CY, Park HC, Lim CO, Kim WB, Harper JF, Cho MJ (2000) Identification of a calmodulin-regulated soybean Ca^{2+}-ATPase (SCA1) that is located in the plasma membrane. Plant Cell 12(8):1393–1407

Clough SJ, Bent AF (1998) Floral dip: a simplified method for Agrobacterium-mediated transformation of *Arabidopsis thaliana*. Plant J 16(6):735–743

Cunningham KW, Fink GR (1994) Calcineurin-dependent growth control in *Saccharomyces cerevisiae* mutants lacking PMC1,

a homolog of plasma membrane Ca^{2+} ATPases. J Cell Biol 124(3):351–363

Curran AC, Hwang I, Corbin J, Martinez S, Rayle D, Sze H, Harper JF (2000) Autoinhibition of a calmodulin-dependent calcium pump involves a structure in the stalk that connects the transmembrane domain to the ATPase catalytic domain. J Biol Chem 275(39):30301–30308. doi:10.1074/jbc.M002047200

De Michelis MI, Carnelli A, Rasi-Caldogno F (1993) The Ca^{2+} pump of the plasma membrane of *Arabidopsis thaliana*: characteristics and sensitivity to fluorescein derivatives. Bot Acta 106(1):20–25

Dodd AN, Kudla J, Sanders D (2010) The language of calcium signaling. Annu Rev Plant Biol 61:593–620. doi:10.1146/annurev-arplant-070109-104628

Frei dit Frey N, Mbengue M, Kwaaitaal M, Nitsch L, Altenbach D, Häweker H, Lozano-Duran R, Njo MF, Beeckman T, Huettel B, Borst JW, Panstruga R, Robatzek S (2012) Plasma membrane calcium ATPases are important components of receptor-mediated signaling in plant immune responses and development. Plant Physiol 159(2):798–809. doi:10.1104/pp.111.192575

Fusca T, Bonza MC, Luoni L, Meneghelli S, Marrano CA, De Michelis MI (2009) Single point mutations in the small cytoplasmic loop of ACA8, a plasma membrane Ca^{2+}-ATPase of *Arabidopsis thaliana*, generate partially deregulated pumps. J Biol Chem 284(45):30881–30888. doi:10.1074/jbc.M109.006148

Geisler M, Axelsen KB, Harper JF, Palmgren MG (2000a) Molecular aspects of higher plant P-type Ca^{2+}-ATPases. Biochim Biophys Acta 1465(1–2):52–78

Geisler M, Frangne N, Gomes E, Martinoia E, Palmgren MG (2000b) The ACA4 gene of *Arabidopsis* encodes a vacuolar membrane calcium pump that improves salt tolerance in yeast. Plant Physiol 124(4):1814–1827

George L, Romanowsky SM, Harper JF, Sharrock RA (2008) The ACA10 Ca^{2+}-ATPase regulates adult vegetative development and inflorescence architecture in *Arabidopsis*. Plant Physiol 146(2):716–728. doi:10.1104/pp.107.108118

Giacometti S, Marrano CA, Bonza MC, Luoni L, Limonta M, De Michelis MI (2012) Phosphorylation of serine residues in the N-terminus modulates the activity of ACA8, a plasma membrane Ca^{2+}-ATPase of *Arabidopsis thaliana*. J Exp Bot 63(3):1215–1224. doi:10.1093/jxb/err346

Gish LA, Clark SE (2011) The RLK/Pelle family of kinases. Plant J 66(1):117–127. doi:10.1111/j.1365-313X.2011.04518.x

Gourdon P, Andersen JL, Hein KL, Bublitz M, Pedersen BP, Liu XY, Yatime L, Nyblom M, Nielsen TT, Olesen C, Møller JV, Nissen P, Morth JP (2011) HiLiDe-systematic approach to membrane protein crystallization in lipid and detergent. Cryst Growth Des 11(6):2098–2106. doi:10.1021/Cg101360d

Harper JF, Hong B, Hwang I, Guo HQ, Stoddard R, Huang JF, Palmgren MG, Sze H (1998) A novel calmodulin-regulated Ca^{2+}-ATPase (ACA2) from *Arabidopsis* with an N-terminal autoinhibitory domain. J Biol Chem 273(2):1099–1106

Hellens RP, Edwards EA, Leyland NR, Bean S, Mullineaux PM (2000) pGreen: a versatile and flexible binary Ti vector for Agrobacterium-mediated plant transformation. Plant Mol Biol 42(6):819–832

Hong B, Ichida A, Wang Y, Gens JS, Pickard BG, Harper JF (1999) Identification of a calmodulin-regulated Ca^{2+}-ATPase in the endoplasmic reticulum. Plant Physiol 119(4):1165–1176

Hwang I, Harper JF, Liang F, Sze H (2000) Calmodulin activation of an endoplasmic reticulum-located calcium pump involves an interaction with the N-terminal auto inhibitory domain. Plant Physiol 122(1):157–168

Kabala K, Klobus G (2005) Plant Ca^{2+}-ATPases. Acta Physiol Plant 27:559–574

Kudla J, Batistic O, Hashimoto K (2010) Calcium signals: the lead currency of plant information processing. Plant Cell 22(3):541–563. doi:10.1105/tpc.109.072686

Lee SM, Kim HS, Han HJ, Moon BC, Kim CY, Harper JF, Chung WS (2007) Identification of a calmodulin-regulated autoinhibited Ca2+-ATPase (ACA11) that is localized to vacuole membranes in *Arabidopsis*. FEBS Lett 581(21):3943–3949. doi:10.1016/j.febslet.2007.07.023

McAinsh MR, Pittman JK (2009) Shaping the calcium signature. New Phytol 181(2):275–294. doi:10.1111/j.1469-8137.2008.02682.x

Møller JV, Juul B, le Maire M (1996) Structural organization, ion transport, and energy transduction of P-type ATPases. Biochim Biophys Acta 1286(1):1–51

Palmgren MG, Nissen P (2011) P-type ATPases. Annu Rev Biophys 40:243–266. doi:10.1146/annurev.biophys.093008.131331

Pedersen CN, Axelsen KB, Harper JF, Palmgren MG (2012) Evolution of plant p-type ATPases. Front Plant Sci 3:31. doi:10.3389/fpls.2012.00031

Pittman JK, Bonza MC, De Michelis MI (2011) Ca^{2+} pumps and Ca^{2+} antiporters in plant development. In: Geisler M, Venema K (eds) Transporters and pumps in plant signalling. Springer, Berlin, Heidelberg, D, pp 133–161

Ranf S, Eschen-Lippold L, Pecher P, Lee J, Scheel D (2011) Interplay between calcium signalling and early signalling elements during defence responses to microbe- or damage-associated molecular patterns. Plant J 68(1):100–113. doi:10.1111/j.1365-313X.2011.04671.x

Sanders D, Pelloux J, Brownlee C, Harper JF (2002) Calcium at the crossroads of signaling. Plant Cell 14(Suppl):S401–S417

Schiøtt M, Palmgren MG (2005) Two plant Ca^{2+} pumps expressed in stomatal guard cells show opposite expression patterns during cold stress. Physiol Plant 124(2):278–283. doi:10.1111/j.1399-3054.2005.00512.x

Schiøtt M, Romanowsky SM, Baekgaard L, Jakobsen MK, Palmgren MG, Harper JF (2004) A plant plasma membrane Ca^{2+} pump is required for normal pollen tube growth and fertilization. Proc Natl Acad Sci USA 101(25):9502–9507. doi:10.1073/pnas.0401542101

Shiu SH, Bleecker AB (2001) Receptor-like kinases from *Arabidopsis* form a monophyletic gene family related to animal receptor kinases. Proc Natl Acad Sci USA 98(19):10763–10768. doi:10.1073/pnas.181141598

Spalding EP, Harper JF (2011) The ins and outs of cellular Ca^{2+} transport. Curr Opin Plant Biol 14(6):715–720. doi:10.1016/j.pbi.2011.08.001

Sze H, Liang F, Hwang I, Curran AC, Harper JF (2000) Diversity and regulation of plant Ca^{2+} pumps: insights from expression in yeast. Annu Rev Plant Physiol Plant Mol Biol 51:433–462. doi:10.1146/annurev.arplant.51.1.433

Tidow H, Poulsen LR, Andreeva A, Knudsen M, Hein KL, Wiuf C, Palmgren MG, Nissen P (2012) A bimodular mechanism of calcium control in eukaryotes. Nature 491(7424):468–472. doi:10.1038/nature11539

Winter D, Vinegar B, Nahal H, Ammar R, Wilson GV, Provart NJ (2007) An "electronic fluorescent pictograph" browser for exploring and analyzing large-scale biological data sets. PLoS ONE 2(8):e718. doi:10.1371/journal.pone.0000718